On the role of overparameterization in off-policy Temporal Difference learning with linear function approximation

Valentin Thomas
Mila, Université de Montréal
vltn.thomas@gmail.com

Abstract

Much of the recent successes of deep learning can be attributed to scaling up the size of the networks to the point where they often are vastly overparameterized. Thus, understanding the role of overparameterization is of increasing importance. While predictive theories have been developed for supervised learning, little is known about the Reinforcement Learning case. In this work, we take a theoretical approach and study the role of overparameterization for off-policy Temporal Difference (TD) learning in the linear setting. We leverage tools from random matrix theory and random graph theory to obtain a characterization of the spectrum of the TD operator. We use this result to study the stability and optimization dynamics of TD learning as a function of the number of parameters.

1 Introduction

Occam's razor principle states that among many plausible explanations, the simplest one is the most likely to be true. In statistics and machine learning, this is often interpreted as models with a restricted number of parameters should be privileged as they generalize better [1]. This view is supported by the classical *bias-variance trade-off* which implies that models that are too flexible are bound to overfit [2]. Yet, deep neural networks with more parameters than training data points achieved remarkable performance in many domains [3, 4, 5], challenging this conventional wisdom. A significant understanding of this apparent tension has been reached in recent years. A large body of work using tools from *random matrix theory* has shown that, in models with random features, overparameterization does not lead to overfitting but instead better generalization [6]. This phenomenon is known as *double descent* and unifies the traditional and modern understanding of bias and variance. Importantly, [7] has shown that the double descent phenomenon is in large part explained by purely optimization rather than label noise. Following their insight, we mainly take an optimization approach in the rest of our paper.

While we now have a theory of overparameterization in supervised learning, the theoretical analysis of overparameterization in the reinforcement learning (RL) setting is largely unexplored [8]. Indeed, RL poses several new additional challenges. First, the agent has to interact with an *environment* whose structure may be complex. Second, each state may not be sampled with equal probability while each datapoint is usually sampled uniformly in supervised learning. In this work, we focus mainly on *policy evaluation*, i.e evaluating the expected return of a fixed policy. More precisely, we study the behavior of Temporal Difference learning [9] which has become ubiquitous for policy evaluation in modern Deep RL [10, 11].

Our contributions are, in the limit of large number of states and parameters: **1)** We introduce a class of random graphs for which we can compute analytically the spectrum of the TD operator when using uniform off-policy sampling, **2)** we derive approximations for the largest and smallest

36th Conference on Neural Information Processing Systems (NeurIPS 2022).

eigenvalue in the non-uniform case. Furthermore, we analyze the behavior of the traditional Mean Square Bellman Error (MSBE) when learning with TD(0) and show that **3)** it exhibits a double descent phenomenon similar to supervised learning but with a multiplicative factor depending on the discount factor in the overparameterized regime and **4)** the asymptotic residual MSBE displays a peaking behavior near the interpolation threshold (when the number of parameters approaches the number of states) that is specific to RL. Finally, **5)** we showcase how the non-stationarity of the policy can make the optimization of the value function unstable. All of these points are motivated theoretically and empirically validated on small gridworlds MDPs.

2 Background

2.1 Value estimation

Definition: We place ourselves in the Markov Decision Process (MDP) setting [12] defined by $\{\mathcal{S}, \mathcal{A}, \mathbf{P}_{sa\to s}, \mathbf{r}, \gamma, p_0\}$, where $\mathcal{S}$ and $\mathcal{A}$ denote the finite state and action spaces, $\mathbf{P}_{sa\to s} \in \mathbb{R}^{|\mathcal{S}|\cdot|\mathcal{A}|\times|\mathcal{S}|}$ is the environment transition probability matrix and $\mathbf{r} \in \mathbb{R}^{|\mathcal{S}|\cdot|\mathcal{A}|}$ denotes the (deterministic) reward vector. $\gamma \in [0, 1[$ is the discount factor, and lastly, p_0 is the initial state distribution. For a given *policy* π, i.e a distribution over actions given a state, the goal of value estimation is to be able to estimate the expected discounted return $\mathbf{q}^\pi(s,a) = \mathbb{E}_{\mathbf{P}_{sa\to s},\pi}\big[\sum_t \gamma^t \mathbf{r}(s_t,a_t)|s_0 = s, a_0 = a\big]$. This quantity is also known as the state-action value or the Q-function. Furthermore, it can be written as the solution of the *Bellman equation* [13][1]: $\mathbf{q}^\pi(s,a) = \mathbf{r}(s,a) + \gamma\mathbb{E}_{\mathbf{P}_{sa\to s},\pi}[\mathbf{q}^\pi(s',a')]$. By defining $\mathbf{P}^\pi \in \mathbb{R}^{|\mathcal{S}|\cdot|\mathcal{A}|\times|\mathcal{S}|\cdot|\mathcal{A}|}$ the state-action to state-action transition matrix, we can write it in matrix form

$$\mathbf{q}^\pi = \mathbf{r} + \gamma\mathbf{P}^\pi\mathbf{q}^\pi \tag{1}$$

Linear function approximation: While Equation (1) can be solved efficiently when $\mathbf{r}, \mathbf{P}^\pi$ are known and when $n = |\mathcal{S}|\cdot|\mathcal{A}|$ is not too large, in many cases this cannot be computed. One solution is to introduce a parameter vector $\theta \in \mathbb{R}^p$ and a feature matrix $\Phi \in \mathbb{R}^{n\times p}$ and optimize θ to approximate $\mathbf{q}^\pi$ as $\mathbf{q}^\pi \approx \Phi\theta$. This is referred to as the Linear Function Approximation (LFA) setting.

Temporal Difference with LFA: Estimating the Q-function in the Linear Function Approximation setting can be done using the well-known algorithm TD(0) [9] whose expected update is

$$\theta_{t+1} = \theta_t + \eta\Phi^\top\Xi\big(\mathbf{r} + \gamma\mathbf{P}^\pi\Phi\theta_t - \Phi\theta_t\big) \tag{2}$$

where Ξ is the off-policy distribution matrix, a $n \times n$ diagonal matrix with positive entries summing to 1, weighting each state-action by their probability of being sampled. Contrary to gradient descent with an appropriate step-size, TD(0) is not guaranteed to converge as the matrix $\Phi^\top\Xi\big(\mathbf{I}_n - \gamma\mathbf{P}^\pi\big)\Phi$ might have a negative eigenvalue. This phenomenon is known as the *deadly triad* as it can only happen when we are (i) off-policy, (ii) using function approximation and (iii) bootstrapping on the next value as TD(0) does [14, 15, 16].

2.2 Random Matrix Theory

Wishart matrices: Extremely relevant in the study of least squares with random features are matrices from the *Wishart distribution* [17]. These matrices can be written as $\frac{1}{n}\Phi^\top\Phi$ for Φ a $n \times p$ matrix with entries of zero mean, unit variance and bounded 4th moment sampled independently and identically distributed. In that case, when $p, n \to \infty$ and the ratio converges to a finite limit $\lim_{p,n\to\infty} p/n = \rho \in]0, +\infty[$, the empirical spectral distribution converges to the Marchenko-Pastur [18] (MP) distribution whose density can be written as

$$d\mu(x) = \max\{1 - 1/\rho, 0\}\ 1_{\{0\}}(x)dx + \frac{1}{2\pi\rho x}\sqrt{(x - \lambda^+_{\min})(\lambda_{\max} - x)}\ 1_{[\lambda^+_{\min},\lambda_{\max}]}(x)dx \tag{3}$$

where $1_A(\cdot)$ is the indicator function, valued at 1 if $x \in A$, 0 otherwise and $\max\{1 - 1/\rho, 0\}\ \delta_{\{0\}}(x)$ are the 0 eigenvalues, which exist when $p \geq n$, $\lambda_{\max} = (1 + \sqrt{\rho})^2$, the largest, and $\lambda^+_{\min} = (1 - \sqrt{\rho})^2$, the smallest non-zero eigenvalue.

[1] Note that we study here the expectation Bellman equation, not the optimality Bellman equation which would feature a $\max$ operator over the next action.

Wigner-type matrices: [19] historically introduced and studied symmetric $n \times n$ matrices of the form $\mathbf{W}$ where $\mathbf{W}_{ij}, i \geq j$ are sampled i.i.d from a law of mean 0 and unit variance for $i \geq j$[2]. $\frac{1}{\sqrt{n}}\mathbf{W}$ has a real spectrum which converges to the *semi-circle* distribution $d\mu(x) = \frac{1}{2\pi}\sqrt{4-x^2}\ 1_{[-2,2]}dx$. When non-symmetric, the spectrum converges to the complex unit disk$\{z \in \mathbb{C}, |z| \leq 1\}$[3] [21].

2.3 Random graphs

Random graphs are useful models to infer structural or spectral properties of typical graphs. The earliest theoretical analyses of random graphs that we are aware of were done independently by [22] and [23]. The model introduced in [22] is a random graph where each of the n nodes is connected at random to d others. The second model [23] is slightly different as each node is independently connected to any other with a probability $\mu \in]0, 1[$. We refer to the first one as the d-regular Erdős-Rényi model $\mathbb{G}(n, d)$ and the second one as the Erdős-Rényi-Gilbert $\mathbb{G}(n, \mu)$ model.

Given the adjacency matrix $\mathbf{A}$, with $\mathbf{A}_{ij} = 1$ if i is connected to j, it is possible to construct a matrix $\mathbf{P}$ by renormalizing the rows of $\mathbf{A}$ so that $\mathbf{P}$ is a stochastic matrix (positive entries and rows summing to 1). $\mathbf{P}$ corresponds to the Markov transition matrix of a random walk on the graph and is connected to the *(left)-normalized Laplacian* $\mathbf{L}$ by $\mathbf{L} = \mathbf{I}_n - \mathbf{P}$. For many classes of random graphs, the spectrum of these quantities is known [24, 25].

3 Spectrum of TD: from random graphs to spiked models

3.1 From Ordinary Least Squares to TD(0)

Random matrix models have been used in supervised learning, especially in the simple least squares model [26, 27, 28], to explain phenomena arising in deep learning. Indeed, while much simpler than large neural networks, these models can shed light on the optimization and generalization behavior of vastly overparameterized models [29, 30], something that most traditional complexity measures could not [31, 32].

Using gradient descent on a least square problem, our parameter update can be written as

$$\theta_{t+1} - \theta^* = \big(\mathbf{I}_p - \eta\Phi^\top\Phi\big)(\theta_t - \theta^*) \tag{4}$$

for $\Phi : \mathbb{R}^{n\times p}$ the feature matrix and θ^* the solution found by gradient descent. When choosing the learning rate η optimally, the convergence rate is expressed as $\frac{\lambda_{\max}/\lambda^+_{\min}-1}{\lambda_{\max}/\lambda^+_{\min}+1}$ for $\lambda^+_{\min}$, respectively $\lambda_{\max}$, the smallest, resp. largest, non-zero eigenvalue of $\Phi^\top\Phi$ [33].

When Φ has i.i.d entries with zero mean, unit variance and bounded 4th moment, as we will consider in the rest of this paper, $\frac{1}{n}\Phi^\top\Phi$ follows the Wishart distribution. In particular, we have analytical expressions for the asymptotic minimum and maximum eigenvalue (section 2.2). When $\lim_{p,n\to\infty} p/n = \rho$, we have $\lambda_{\max}/\lambda^+_{\min} \to \left(\frac{1+\sqrt{\rho}}{1-\sqrt{\rho}}\right)^2 \geq 1$. This function has asymptotes at 1, for $p = o(n)$ or $n = o(p)$ and diverges when $n = p$. This peak-shaped function can also be observed empirically in more complex models such as kernel methods [34] and neural networks in the limit of infinite width as they are in the Neural Tangent Kernel regime [35, 36].

However, when using TD(0), presented in section 2.1, the feature covariance matrix $\Phi^\top\Phi$ would be replaced by $\Phi^\top\Xi(\mathbf{I}_n - \gamma\mathbf{P}^\pi)\Phi$. While [8] derived worst-case bounds for overparameterized TD, their dependency of the overparamerization ratio $\rho = p/n$ is not obvious. In this work we chose to use tools for *random matrix theory* for modeling the behavior of TD. While we can model Φ as an i.i.d matrix, it is not obvious how to model Ξ and $\mathbf{P}^\pi$ in a realistic manner that would still allow us to characterize the spectrum of the TD operator $\Phi^\top\Xi(\mathbf{I}_n - \gamma\mathbf{P}^\pi)\Phi$. For general Ξ and $\mathbf{P}^\pi$ no closed form solution for the spectrum exists. We believe this is one of the key reasons why overparameterization in Temporal Difference learning has not been studied extensively. Thus, finding good typical models for $\mathbf{P}^\pi$ is of utmost importance, and the next section will introduce a class of models for which the spectrum of TD can be computed.

[2] and an additional light tail decay condition, weaker than the bounded 4-th moment one [20].

[3] both in probability and almost surely.

3.2 $\mathbf{P}^\pi$ as the Markov transition matrix of a random graph

In RL, $\mathbf{P}^\pi$ is the Markov transition matrix of a random walk when sampling from π. We will assume in the rest of the paper that the Markov chain is irreducible and aperiodic so that $\mathbf{P}^\pi$ has a unique stationary distribution denoted $\mathbf{d}_\pi$.

As we wish to understand the expected behavior of the TD algorithm, we propose in this subsection a simple yet expressive model of $\mathbf{P}^\pi$ that will allow us to do so. As random graphs are used to model properties of typical graphs, a candidate for a model of $\mathbf{P}^\pi$ would be to take the Markov transition matrix of a random graph. However, random graphs, at least the Erdős-Rényi(-Gilbert) type ones, are not able natively to take into account the impact of π, most importantly the fact that some state-actions are visited more often than others under $\mathbf{d}_\pi$, the stationary distribution of π. In this subsection, we propose a simple model for $\mathbf{P}^\pi$, denoted by $\hat{\mathbf{P}}^\pi$, which is the Markov transition matrix of a $\mathbb{G}(n, \mu)$ graph *deformed* by $\mathbf{d}_\pi$.

Let us start with an undirected graph of the type $\mathbb{G}(n, \mu)$. To take into account the state-action visitation $\mathbf{d}_\pi$, we construct the diagonal matrix $\mathbf{D}_\pi$ so that $\mathbf{D}_\pi = \texttt{diag}(\mathbf{d}_\pi)$. Now, we define the deformed adjacency matrix $\mathbf{A}^\pi$ as $\mathbf{A}^\pi \triangleq n\mathbf{A}\mathbf{D}_\pi$ where $\mathbf{A}$ is the original adjacency matrix. When $\mathbf{d}_\pi$ is uniform, we revert back to the original case $\mathbf{A}^\pi = \mathbf{A}$. This construction keeps the same edges as in the original graph but re-weights them by how likely $\mathbf{d}_\pi$ would visit that state-action. We can informally write the Markov transition matrix associated with this deformed graph as[4] $\hat{\mathbf{P}}^\pi = \mathbf{1}_n\mathbf{d}_\pi^\top + \mathbf{X}^\pi$ where (i) $\mathbf{1}_n\mathbf{d}_\pi^\top$ is a deterministic rank one matrix associated to the eigenvalue 1 as $\mathbf{1}_n^\top\mathbf{d}_\pi = 1$ and (ii) $\mathbf{X}^\pi = \sqrt{\frac{n(1-\mu)}{\mu}}\frac{1}{\sqrt{n}}\mathbf{W}\mathbf{D}_\pi$ is a stochastic matrix of null expectation as $\frac{1}{\sqrt{n}}\mathbf{W}$ is a Wigner-type matrix with zero mean and unit variance. It can be tempting to understand under which conditions the stochastic part becomes negligible and what it entails. As we will see shortly, this setting will reveal itself to be of importance when studying the spectrum of TD.

Definition 1 (Asymptotically well-connected graphs)**.** *We say a graph $\mathbb{G}$ is asymptotically well-connected if $|\lambda_2| \in o(1)$ for $1 = \lambda_1 \geq |\lambda_2| \geq \cdots \geq |\lambda_n|$ the (modulus) ordered eigenvalues of its Markov transition matrix.*

The choice for the name of Definition 1 comes from the fact that the second smallest eigenvalue of the Laplacian is related to the presence of *bottlenecks* in the graph through Cheeger's inequality [37].

Example. Graphs of the type $\mathbb{G}(n, \mu)$ (resp. $\mathbb{G}(n, d)$) are asymptotically well-connected if their expected degree $d = n\mu$ (resp. d) grows to $+\infty$ with n, i.e $1 \in o(d)$ [24, 25].

Proposition 3.1. *For the $\mathbf{d}_\pi$-deformed $\mathbb{G}(n, \mu)$ graph studied above, assuming $\hat{\mathbf{P}}^\pi = \mathbf{1}_n\mathbf{d}_\pi^\top + \mathbf{X}^\pi$, then the graph is asymptotically well-connected if $n\|\mathbf{d}_\pi\|_\infty \in o(\sqrt{d})$.*

This again generalizes the uniform case as, when $\mathbf{d}_\pi$ is uniform, the condition becomes equivalent to $1 \in o(d)$ as in the example. In the non-uniform case, this condition entails that either $\mathbf{d}_\pi$ spreads efficiently across states, or the degree d rises fast enough that those states are still visited sufficiently often. Note that the *asymptotically well-connected* condition is also satisfied if we use longer back-ups of length k such that k grows with n to $+\infty$, i.e $1 \in o(k)$ for the TD update. See Lemma B.2 for details.

In those cases, we have

$$\boxed{\hat{\mathbf{P}}^\pi = \mathbf{1}_n\mathbf{d}_\pi^\top + o(1)} \tag{5}$$

This approximation is particularly interesting as it asymptotically conserves the left and right eigenvectors, $\mathbf{d}_\pi$ and $\mathbf{1}_n$, of the original $\mathbf{P}^\pi$ associated to the eigenvalue 1. Furthermore, if all state-actions are reachable, the sequence of matrix power iterates of $\mathbf{P}^\pi$, $\left(\mathbf{P}^\pi\right)^k$ converges to $\mathbf{1}_n\mathbf{d}_\pi^\top$. While we are not the first to use tools from graph theory in the context of RL, related works we are aware of [38, 39, 40, 41] take a different approach and leverage eigenvectors of the Markov transition matrix (or Laplacian) to construct better representations for the value function or use them as options. In contrast, we use spectral properties of $\mathbf{P}^\pi$ to study the convergence of Temporal Difference learning.

[4] Derivation can be found in Appendix.

3.3 Spiked Wishart model for TD with uniform sampling

Now that we have a simple random graph model for $\mathbf{P}^\pi$, we focus on estimating the spectrum of $\Phi^\top \Xi(\mathbf{I}_n - \gamma \hat{\mathbf{P}}^\pi)\Phi$. For simplicity, we assume the off-policy sampling is done uniformly, i.e $\Xi = \frac{1}{n}\mathbf{I}_n$. While this assumption is not realistic in most RL settings, it is still of interest in the context of dynamic programming where we have access to all the states.

Proposition 3.2 (Spiked MP)**.** *If $\rho\gamma^2 < 1$ the spectrum of $\frac{1}{n}\Phi^\top(\mathbf{I}_n - \gamma\hat{\mathbf{P}}^\pi)\Phi$ converges to the Marchenko-Pastur law with parameter ρ. When $\rho\gamma^2 \geq 1$, there is a phase transition [42] for the minimum non-zero eigenvalue $\lambda^+_{\min}$ which separates from bulk and converges to*

$$\boxed{\lambda^+_{\min} \xrightarrow[p/n\to\rho]{a.s} \lambda^{spiked} = (1-\gamma)(\rho - \tfrac{1}{\gamma})} \tag{6}$$

Note that the phase transition is smooth as for $\rho = 1/\gamma^2$, $\lambda^{spiked} = (\sqrt{1/\gamma^2} - 1)^2$.

Vast overparameterization and tabular case: An interesting regime is when $\rho \gg \frac{1}{\gamma^2} > 1$. In that case, the maximum eigenvalue of the MP law and the spiked one differ by a factor $H = \frac{1}{1-\gamma}$, the *effective horizon* of the problem, as $\lim_{\rho\to\infty} \lambda_{\max}/\lambda^+_{\min} = \frac{1}{1-\gamma}$. In the tabular regime, $\Phi = \mathbf{I}_n$. As $\mathbf{P}^\pi$ has eigenvalues in $[-1, 1]$, the eigenvalues of $\mathbf{I}_n - \gamma\mathbf{P}^\pi$ are in $[1-\gamma, 1+\gamma]$. This would give a worst case ratio of $\frac{1+\gamma}{1-\gamma}$ which, up to a factor $1+\gamma \leq 2$, is the same as the vastly overparameterized case above. As these eigenvalues govern the optimization speed of TD, the vastly overparameterized case and the tabular can be thought of as comparable.

3.4 Non-uniform off-policy sampling

In the previous subsection we were able to characterize the spectrum of $\Phi^\top\Xi(\mathbf{I}_n - \gamma\hat{\mathbf{P}}^\pi)\Phi$ assuming $\Xi = \frac{1}{n}\mathbf{I}_n$. In this subsection we analyze the more general case where Ξ is not uniform. However by doing so, we lose guarantees and must resort to approximations. First, we analyze the eigenvalues of $\Xi(\mathbf{I}_n - \gamma\hat{\mathbf{P}}^\pi)$, or rather, in the limit of large n, the eigenvalues of $\Xi(\mathbf{I}_n - \gamma\mathbf{1}_n\mathbf{d}_\pi^\top)$.

Lemma 3.1. *If $\Xi = \texttt{diag}(\xi_1, \ldots, \xi_n)$ is non-singular, the eigenvalues of $\Xi(\mathbf{I}_n - \gamma\mathbf{1}_n\mathbf{d}_\pi^\top)$ satisfy a* secular *equation [43]*

$$1 - \gamma\sum_{i=1}^{n} \frac{\xi_i \cdot \mathbf{d}_\pi(i)}{\xi_i - \lambda} = 0 \tag{7}$$

This expression is another form of the *characteristic polynomial* of a matrix whose roots are its eigenvalues. However, this form enables us to derive approximations more easily. In particular, for the least visited state-action $m = \arg\min_{i=1,\ldots,n} \xi_i$, if $\xi_m \ll \xi_i, i \neq m$, we have for $\lambda \approx \xi_m$ that $\frac{1}{\xi_i - \lambda} \approx \frac{1}{\xi_i}$ if $i \neq m$. From this assumption, we derive an approximation for the minimum eigenvalue of $\Xi(\mathbf{I}_n - \gamma\hat{\mathbf{P}}^\pi)$

$$\ell_{\min} \approx \xi_m \tfrac{1-\gamma}{1-\gamma+\gamma\,\mathbf{d}_\pi(m)} \tag{8}$$

This eigenvalue is inferior to ξ_m and reflects the interaction between the off-policy distribution and the discount factor. At worst, if $\mathbf{d}_\pi$ mostly visits state m, it will be close to $\xi_m(1-\gamma)$ which is the product of the minimum eigenvalues of Ξ and $\mathbf{I}_n - \gamma\hat{\mathbf{P}}^\pi$. A similar expression can be derived for the maximum eigenvalue under similar assumptions.

Now, again reasoning approximately, if that eigenvalue was very small compared to the other ones who would form a bulk of similar values, we could expect $\Phi^\top\Xi(\mathbf{I}_n - \gamma\hat{\mathbf{P}}^\pi)\Phi$ to have a similar spiking behavior as before. However, in that case, the spiking eigenvalue would be

$$\lambda^+_{\min} \approx n\ell_{\min}\big(\rho - \tfrac{1}{1-n\ell_{\min}}\big) \tag{9}$$

While less simple than the estimators developed in the last subsection, we will see in Section 5 that it still accurately predicts the smallest non-zero eigenvalue.

4 Optimizing with Temporal Difference learning

4.1 Decomposition of the error

Using results about the spectrum of the TD operator shown in the last section, we analyze the behavior of the Mean Square Bellman Error $\mathcal{L}_{MSBE}(\mathbf{q}_t) = \frac{1}{2}\|\mathbf{r} + \gamma \mathbf{P}^\pi \mathbf{q}_t - \mathbf{q}_t\|_\Xi^2$ during the optimization. In particular, assuming $\Phi^\top \Xi(\mathbf{I}_n - \gamma \mathbf{P}^\pi)\Phi$ is non-singular for $p < n$

$$\mathbf{q}_{\text{TD}} = \begin{cases} \Phi\theta_{\text{TD}} = \Phi(\Phi^\top \Xi(\mathbf{I}_n - \gamma \mathbf{P}^\pi)\Phi)^{-1}\Phi^\top \Xi \mathbf{r}, \text{ if } p < n \\ \mathbf{q}^\pi \quad = \quad (\mathbf{I}_n - \gamma \mathbf{P}^\pi)^{-1}\mathbf{r}, \text{ if } p > n \end{cases}$$

the $\mathbf{q}$-value asymptotically reached by TD(0), we can decompose this error into two components.

Lemma 4.1 (Decomposition of the error)**.** *For $\mathbf{q}_t = \Phi\theta_t$, where θ_t is updated with TD(0) (eq. (2)), we have the following decomposition*

$$\|\mathbf{r} + \gamma \mathbf{P}^\pi \mathbf{q}_t - \mathbf{q}_t\|_\Xi \leq \sqrt{n\|\Xi\|_\infty} \cdot \|\mathbf{q}_t - \mathbf{q}_{TD}\|_2 + \|\mathbf{r} + \gamma \mathbf{P}^\pi \mathbf{q}_{TD} - \mathbf{q}_{TD}\|_\Xi \tag{10}$$

where $\|\mathbf{x}\|_\Xi = \sqrt{\mathbf{x}^\top \Xi \mathbf{x}}$ is the 2-norm in metric Ξ.

Following [44], we refer to $\|\mathbf{q}_t - \mathbf{q}_{\text{TD}}\|_2$ as the approximation error and $\|\mathbf{r} + \gamma \mathbf{P}^\pi \mathbf{q}_{\text{TD}} - \mathbf{q}_{\text{TD}}\|_\Xi$ as the estimation error. The factor $\sqrt{n\|\Xi\|_\infty} \geq 1$ comes from bounding the spectral norm of $(\mathbf{I}_n - \gamma \mathbf{P}^\pi)$ in metric Ξ. Beyond this factor, we are not exactly in the same setting as [44] as the asymptotic TD(0) value estimate $\mathbf{q}_{\text{TD}}$ may not be the one reaching the lowest estimation error, as known in the RL community [45]. Indeed, TD(0) finds the minimum of the Mean Square Projected Bellman Error (MSPBE) but not of the MSBE [46]. However in practice it is common to minimize the MSBE as it does not require an expensive projection step.

4.2 The ordinary behavior of the approximation error

In this subsection, we take a look at the approximation error, i.e how efficiently we converge to $\mathbf{q}_{\text{TD}}$.

Proposition 4.1. *Let us assume that $\Phi^\top \Xi(\mathbf{I}_n - \gamma \mathbf{P}^\pi)\Phi$ is diagonalizable as $\mathbf{Q}\Lambda\mathbf{Q}^{-1}$, and that its spectrum is real and positive. Denoting by $\lambda_{\min}^+$ and $\lambda_{\max}$ its smallest non-zero and largest eigenvalues, for $\eta = \frac{2}{\lambda_{\min}^+ + \lambda_{\max}}$*

$$\|\mathbf{q}_t - \mathbf{q}_{TD}\|_2^2 \leq \left(\frac{\lambda_{\max}/\lambda_{\min}^+ - 1}{\lambda_{\max}/\lambda_{\min}^+ + 1}\right)^{2t} K^2 \|\mathbf{q}_0 - \mathbf{q}_{TD}\|_2^2 \tag{11}$$

where $K = \kappa(\Phi)\kappa(\mathbf{Q})$ when $p < n$ and $K = \kappa(\mathbf{Q})$ when $p > n$ where κ is the condition number.

The assumptions above can seem strong however they are verified under our model (cf Section 3.3). This is a slightly more general version of the linear convergence of gradient descent, however, as the TD operator may not be diagonalizable in an orthonormal basis, we incur an additional factor K^2.

4.3 The singular behavior of the estimation error

Now we turn our attention to the second term; the estimation error which is the *residual error* after $T \to +\infty$ steps. In supervised learning, we expect this error to be the usual bias of our algorithm and thus to decrease as p/n increases until $p = n$ for which the bias would reach 0 as it is possible to interpolate the data. However, in reinforcement learning, the behavior of this term can be quite different, in particular it can be non-monotonous.

Proposition 4.2. *Let us assume $\hat{\mathbf{P}}^\pi$ satisfies the well-connected property, i.e that it is asymptotically rank one*

$$\lim_{\substack{n,p\to\infty \\ p/n \to \rho}} \|(\mathbf{I}_n - \gamma \hat{\mathbf{P}}^\pi)\mathbf{q}_{TD} - \mathbf{r}\|_\Xi^2 = \|\Pi_\perp \mathbf{r}\|_\Xi^2 + \frac{2\gamma}{1-\gamma\tilde{\rho}}(\mathbf{d}_\pi^\top \Pi \mathbf{r})(\xi^\top \Pi_\perp \mathbf{r}) + (\frac{\gamma}{1-\gamma\tilde{\rho}})^2 \xi^\top \Pi_\perp \mathbf{1}_n (\mathbf{d}_\pi^\top \Pi \mathbf{r})^2$$

where Π is the orthogonal projector onto the span of Φ in norm Ξ: $\Pi = \Phi(\Phi^\top \Xi \Phi)^{-1}\Phi^\top \Xi$, $\Pi_\perp = \mathbf{I}_n - \Pi$ is its complement, and $\tilde{\rho} = \mathbf{d}_\pi^\top \Pi \mathbf{1}_n$.

When $\gamma = 0$, i.e we just perform reward regression, this is equal to $\|\Pi_\perp \mathbf{r}\|_\Xi^2$ which is exactly the residual error in $\mathbf{r}$ that our representation cannot capture. When $\rho > 1$, $\Pi_\perp = 0$ so the limit is zero as we expect from a model able to interpolate the data. However, there is a behavior here not present in supervised learning. When $\tilde{\rho} \approx 1$, which we can expect when Π is closer to identity, i.e p close to but less than n, a *peaking* behavior of the estimation error can happen.

Replacing Π by its expectation[5] $\rho \mathbf{I}_n$ above can lead to an equation simpler to analyze, albeit biased

$$1_{]0,1]}(\rho)\ (1-\rho)\big(\|\mathbf{r}\|_\Xi^2 + 2\frac{\gamma\rho}{1-\gamma\rho}(\mathbf{d}_\pi^\top \mathbf{r})(\xi^\top \mathbf{r}) + (\mathbf{d}_\pi^\top \mathbf{r})^2(\frac{\gamma\rho}{1-\gamma\rho})^2\big) \tag{12}$$

This phenomenon might appear counter-intuitive as we would expected our error to decrease with p. We provide a few insights to make sense of this. First, when γ increases, so does the scale of the Q-function, so we can expect our errors to get bigger. Second, using random features Φ informally has a *smoothing* effect, stronger when ρ is small, which causes the reduction in magnitude from $\frac{1}{1-\gamma}$ to $\frac{1}{1-\gamma\rho}$. This can be observed in the proof in appendix. Finally, peaking behaviors of TD such as this one have been observed in the community [45] but not theoretically explained in a general setting as far as we know.

4.4 Beyond stationary sampling

Until now, we always mentioned n as the number of state-action pairs with the assumption that Ξ was non-singular, i.e that our off-policy sampling *visited all the states*. Here, we take a closer look at what happens when this is not the case. In particular, we study a simple toy model where we assume Ξ only visits $n_{\text{vis}}(t)$ states at time t with uniform probability. This simply changes all the n by $n_{\text{vis}}(t)$ in the previous results. As often observed during training, at $t = 0$, π might start as a more exploratory policy ($n_{\text{vis}}(t = 0)$ high) and over time converges on a more deterministic solution ($n_{\text{vis}}(t)$ low). This can be problematic when performing TD learning with a fixed stepsize η. In that case, under the spiked model developed in Section 3.3 we need to ensure $\eta \leq {}^2/\big(1+\sqrt{p/n_{\text{vis}}(t)}\big)^2 \to {}^2/\lambda_{\max}$ or equivalently

$$n_{\text{vis}}(t) \geq {}^p/\big(\sqrt{\tfrac{2}{\eta}}-1\big)^2 \tag{13}$$

As $n_{\text{vis}}(t)$ can typically decrease, **this condition can be broken and thus TD learning will diverge**. We conjecture this phenomenon may be related to the popularity of adaptive step size methods in RL over fixed step size ones.

5 Experiments

In all the experiments we use Φ i.i.d with normal entries. Per the universality property, our theoretical results hold for all distributions satisfying the hypotheses in Section 2.2.

Study of the spectral distribution: On Figure 1, we validate the theory and approximations of Section 3. For an asymmetric random graph $n = 4000, \mu = {}^1/_2$, the spectrum of $\mathbf{P}$ (a) has an eigenvalue at 1 and the rest of order ${}^1/\sqrt{n}$ [48]. As predicted, the spectrum of the TD operator matches closely a spiked MP distribution (b). When the graph does not satisfy the well-connected property, for instance on a 4 rooms domain ($n = 4096$, π stochastic[6]) (c) the spectral distribution is more complex (d). The relative error on $\lambda_{\min}^+$ is respectively 0.3% and 2%. Despite this, we show that the empirical and theoretical (eq. (9)) values for $\lambda_{\min}^+$ and $\lambda_{\max}$ on the 4 rooms domain ($n = 256$) closely match, both for Ξ uniform or highly ill-conditioned with evenly spaced ξ_i so that $\frac{\max_i \xi_i}{\min_i \xi_i} = 2000$. While (b) and (d) show how violating the *asymptotically well-connected* property breaks our spiked MP distribution result, we show on (e) and (f) that the extreme eigenvalues, which are the ones that matter for our optimization results, are still well predicted, even in more complex settings.

Optimization behavior of TD: On Figure 2 we discuss the results of Section 4. We use again a 4 rooms domain with a fixed stochastic policy and study the Bellman error during training. On all subfigures of Figure 2, we observe that for $\rho \gg 1$ or $\rho \ll 1$, the optimization is faster as the curves for low T are much closer to the asymptotic solution $T = +\infty$ (computed analytically) than for

[5] when $\Xi = \frac{1}{n}\mathbf{I}_n$, by rotational invariance of Φ, we $\mathbb{E}[\Pi] = \rho \mathbf{I}_n$, thus $\mathbb{E}[\tilde{\rho}] = \rho$.

[6] We sampled $\pi(a|s) \sim \text{Uniform}[0, 1]$ and renormalized.

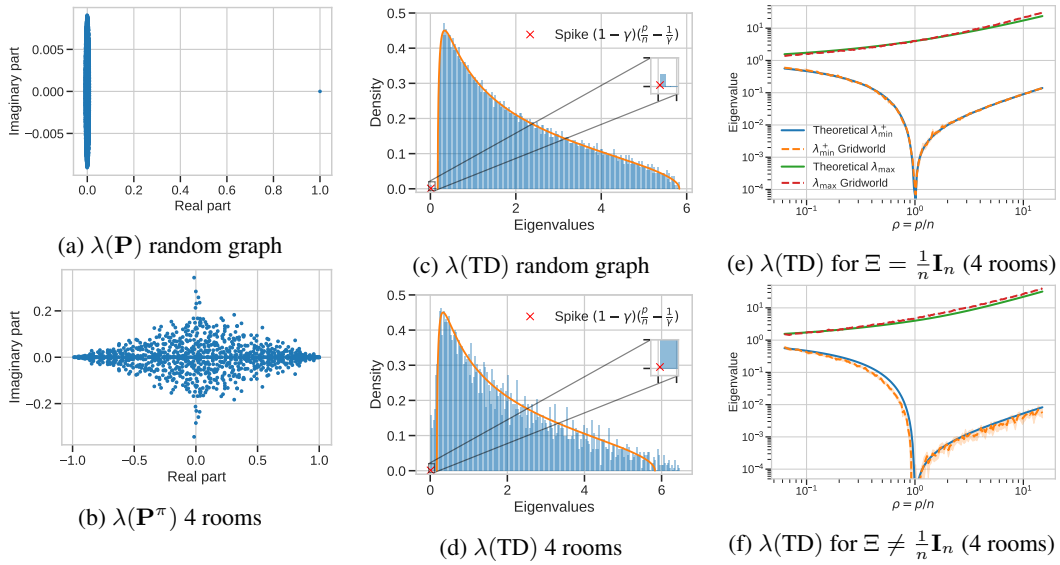

(a) $\lambda(\mathbf{P})$ random graph

(b) $\lambda(\mathbf{P}^\pi)$ 4 rooms

(c) $\lambda(\text{TD})$ random graph

(d) $\lambda(\text{TD})$ 4 rooms

(e) $\lambda(\text{TD})$ for $\Xi = \frac{1}{n}\mathbf{I}_n$ (4 rooms)

(f) $\lambda(\text{TD})$ for $\Xi \neq \frac{1}{n}\mathbf{I}_n$ (4 rooms)

Figure 1: (a) and (b): scatterplot of the spectra of the Markov transition matrix for a $\mathbb{G}(n, \mu)$ graph and the 4 rooms domain. (c) and (d): spectral distribution for the TD operator for $\rho = 2$. When the well-connected assumption is verified (a), the spectral distribution is a spiked ($\times$) Marchenko-Pastur (MP) law (in orange) (c). When the assumption is violated and $\hat{\mathbf{P}}^\pi \not\approx \mathbf{1}_n \mathbf{d}_\pi^\top$ (b), the distribution bleeds out of the MP support, yet the minimum eigenvalue is still close to the spike (d). On (e) and (f) we compare our prediction of the extreme eigenvalues $\lambda^+_{\min}$ and $\lambda_{\max}$ of the TD operator on the 4 rooms domain [47] (b) as a function of p/n. We plot the empirical extreme eigenvalues (dotted) vs (e) MP theoretical ones (eqs. 3, 6) for Ξ uniform and (f) approximation in eq. (9) for Ξ non-uniform. Shaded areas are a 95% confidence interval when randomizing Φ and π (10 seeds).

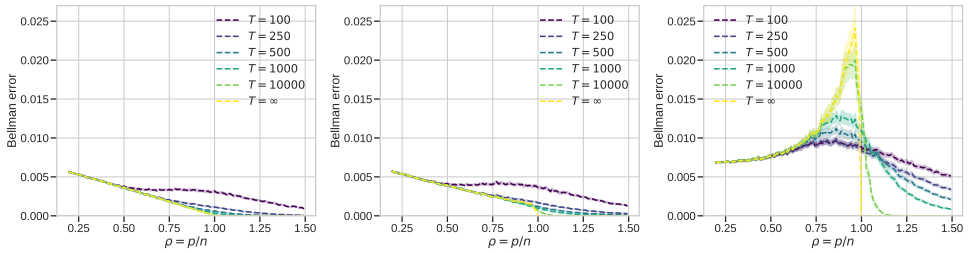

(a) $\gamma = 0.1$, $\mathbf{d}_\pi^\top \mathbf{r} \approx 0.08$

(b) $\gamma = 0.98$, $\mathbf{d}_\pi^\top \mathbf{r} \approx 0.02$

(c) $\gamma = 0.98$, $\mathbf{d}_\pi^\top \mathbf{r} \approx 0.07$

Figure 2: Value of the MSBE as a function of the ratio p/n for various iterations T during optimization. $T = +\infty$ corresponds to the asymptotic solution found by TD(0) (eq. (10)). We use uniform sampling ($\Xi = \frac{1}{n}\mathbf{I}_n$). On (a), for low γ we observe a behavior similar to supervised learning where the residual error decreases and reaches 0 at $p = n$. (b) displays a similar behavior as the term $\mathbf{d}_\pi^\top \mathbf{r}$ is small. (c) As $\mathbf{d}_\pi^\top \mathbf{r}$ is higher, the *peaking* terms $\frac{1}{1-\gamma\bar{\rho}}$ are non-negligible. Shaded areas are a 99% confidence interval over randomness of θ_0 and Φ (100 seeds).

$\rho \approx 1$. This is in line with the result of section 4.2 for a spiked model: the ratio of eigenvalues which governs the optimization speed is $\lambda_{\max}/\lambda^+_{\min} \to 1$ for $\rho \ll 1$ and to $\frac{1}{1-\gamma}$ for $\rho \gg 1$ while it diverges for $\rho \to 1$. This leads to a classical *double descent* phenomenon on (a) and (b) purely due to optimization as predicted by [7]. On (a) and (b) because either γ or $\mathbf{d}_\pi^\top \mathbf{r}$ is small, the terms of order $\frac{1}{1-\gamma\bar{\rho}}$ are negligible and thus it behaves similarly to supervised learning. On (c), the term $\frac{1}{1-\gamma\bar{\rho}}$ dominates and we observe the peaking behavior of the estimation error (Section 4.3). Furthermore on Figure 4 in appendix we study how our model and its approximation of Section 3.3 match the observed peaking behavior.

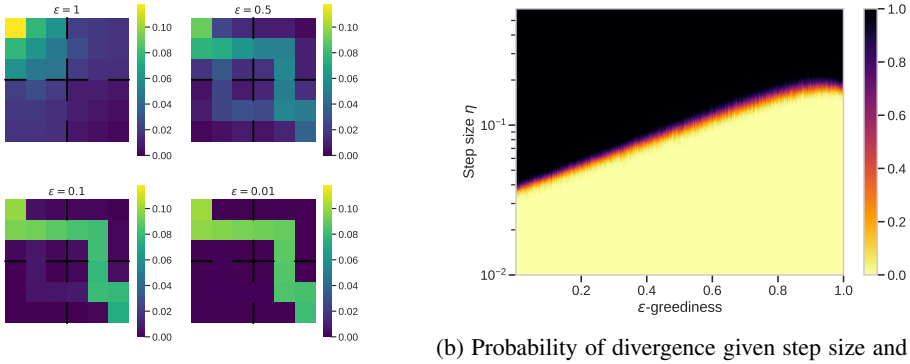

(a) $\mathbf{d}_\pi$ on 4 rooms for different ϵ.

(b) Probability of divergence given step size and ϵ-greediness.

Figure 3: (a): Example of the discounted state distribution in a small 4 rooms domain for varying ϵ-greedy policies. (b) The probability of divergence of TD as a function of the step size η and the ϵ-greediness. For each point we report the probability it leads to divergence computed over 100 random Φ: from yellow (0%) to black (100%).

Stability and non-stationarity: On Figure 3 we highlight how Ξ can affect the convergence of TD ($p = 200$). For this, we use a small 4 rooms ($n = 144$) environment[7] and compute an optimal deterministic policy π^*. Then, by varying the ϵ of a ϵ-greedy policy based on π^*, we can analyze which combination of step size η and ϵ would lead to convergence. On (a), we show the discounted state distribution for various ϵ where larger ϵ lead to more exploration. While our theoretical argument in Section 4.4 was about the number of visited states, we take here a more general and realistic approach where the state visitation is controlled by the greediness of our policy. Typically, during the optimization of a value based method, ϵ is annealed to 0 and the policy becomes more deterministic. On (b) we show the probability of diverging (averaged over 100 samples of Φ) measured by computing the spectral radius of our iteration matrix. As predicted, for a fixed η, when ϵ decreases, we might go through a phase transition where the TD iteration, stable at the beginning, becomes unstable.

6 Conclusion

In this work, we have analyzed the spectral distribution of the Temporal Difference operator when using random features and modeling the Markov transition matrix as the one of a random graph. This characterization allowed us to make predictive theories for the optimization error and stability of TD. Notably we are able to predict how fast we converge and whether the solution found is accurate as a function of the ratio between the number of parameters and the number of state-action pairs. In particular, we highlighted and theoretically explained several phenomena specific to reinforcement learning such as the peaking behavior of the estimation error of TD or how changing the policy might cause divergence when using a fixed step size, even in the *on-policy* setting.

Important directions for future work include: (i) improving the model for $\mathbf{P}^\pi$ through careful analysis of more expressive random graphs, (ii) derive non-asymptotic results using the fluctuations of the extreme eigenvalues of the MP law [42] (iii) extend our results to neural networks in the Neural Tangent Kernel regime and finally (iv) study the behavior of policy optimization algorithms.

Acknowledgments

We thank Alexandre Piché for useful comments on an earlier version of this paper.

References

[1] Hirotugu Akaike. A new look at the statistical model identification. *IEEE transactions on automatic control*, 19(6):716–723, 1974.

[7] where the bottom right state with a reward of 1 leads back to the initial state on the top left.

[2] Stuart Geman, Elie Bienenstock, and René Doursat. Neural Networks and the Bias/Variance Dilemma. *Neural Computation*, 4(1):1–58, 01 1992.

[3] Y. LeCun, B. Boser, J. S. Denker, D. Henderson, R. E. Howard, W. Hubbard, and L. D. Jackel. Backpropagation applied to handwritten zip code recognition. *Neural Computation*, 1(4):541–551, 1989.

[4] Alex Krizhevsky, Ilya Sutskever, and Geoffrey E Hinton. Imagenet classification with deep convolutional neural networks. In F. Pereira, C.J. Burges, L. Bottou, and K.Q. Weinberger, editors, *Advances in Neural Information Processing Systems*, volume 25. Curran Associates, Inc., 2012.

[5] Jacob Devlin, Ming-Wei Chang, Kenton Lee, and Kristina Toutanova. Bert: Pre-training of deep bidirectional transformers for language understanding. *arXiv preprint arXiv: Arxiv-1810.04805*, 2018.

[6] Mikhail Belkin, Daniel Hsu, and Ji Xu. Two models of double descent for weak features. *SIAM Journal on Mathematics of Data Science*, 2(4):1167–1180, 2020.

[7] Ilja Kuzborskij, Csaba Szepesvári, Omar Rivasplata, Amal Rannen-Triki, and Razvan Pascanu. On the role of optimization in double descent: A least squares study. *Advances in Neural Information Processing Systems*, 34, 2021.

[8] Chenjun Xiao, Bo Dai, Jincheng Mei, Oscar A Ramirez, Ramki Gummadi, Chris Harris, and Dale Schuurmans. Understanding and leveraging overparameterization in recursive value estimation. In *International Conference on Learning Representations*, 2021.

[9] Richard S Sutton. Learning to predict by the methods of temporal differences. *Machine learning*, 3(1):9–44, 1988.

[10] Volodymyr Mnih, Koray Kavukcuoglu, David Silver, Alex Graves, Ioannis Antonoglou, Daan Wierstra, and Martin Riedmiller. Playing atari with deep reinforcement learning. *arXiv preprint arXiv:1312.5602*, 2013.

[11] Tuomas Haarnoja, Aurick Zhou, Pieter Abbeel, and Sergey Levine. Soft actor-critic: Off-policy maximum entropy deep reinforcement learning with a stochastic actor. In *International conference on machine learning*, pages 1861–1870. PMLR, 2018.

[12] Martin L Puterman. *Markov decision processes: discrete stochastic dynamic programming*. John Wiley & Sons, 2014.

[13] Richard Bellman. The theory of dynamic programming. *Bulletin of the American Mathematical Society*, 60(6):503–515, 1954.

[14] Leemon Baird. Residual algorithms: Reinforcement learning with function approximation. In *Machine Learning Proceedings 1995*, pages 30–37. Elsevier, 1995.

[15] John N Tsitsiklis and Benjamin Van Roy. Analysis of temporal-diffference learning with function approximation. In *Advances in neural information processing systems*, pages 1075–1081, 1997.

[16] Hado Van Hasselt, Yotam Doron, Florian Strub, Matteo Hessel, Nicolas Sonnerat, and Joseph Modayil. Deep reinforcement learning and the deadly triad. *arXiv preprint arXiv:1812.02648*, 2018.

[17] John Wishart. The generalised product moment distribution in samples from a normal multivariate population. *Biometrika*, pages 32–52, 1928.

[18] Vladimir A Marčenko and Leonid Andreevich Pastur. Distribution of eigenvalues for some sets of random matrices. *Mathematics of the USSR-Sbornik*, 1(4):457, 1967.

[19] Eugene P. Wigner. Characteristic vectors of bordered matrices with infinite dimensions. *Annals of Mathematics*, 62(3):548–564, 1955.

[20] Terence Tao and Van Vu. Random matrices: The universality phenomenon for wigner ensembles. *arXiv preprint arXiv: Arxiv-1202.0068*, 2012.

[21] Terence Tao, Van Vu, and Manjunath Krishnapur. Random matrices: Universality of esds and the circular law. *The Annals of Probability*, 38(5):2023–2065, 2010.

[22] Paul Erdős, Alfréd Rényi, et al. On the evolution of random graphs. *Publ. Math. Inst. Hung. Acad. Sci*, 5(1):17–60, 1960.

[23] Edgar N Gilbert. Random graphs. *The Annals of Mathematical Statistics*, 30(4):1141–1144, 1959.

[24] Yufei Zhao. Spectral distributions of random graphs. 2012.

[25] Linh Tran, Van Vu, and Ke Wang. Sparse random graphs: Eigenvalues and eigenvectors. *arXiv preprint arXiv: Arxiv-1011.6646*, 2010.

[26] Yann Le Cun, Ido Kanter, and Sara A. Solla. Eigenvalues of covariance matrices: Application to neural-network learning. *Phys. Rev. Lett.*, 66:2396–2399, May 1991.

[27] Trevor Hastie, Andrea Montanari, Saharon Rosset, and Ryan J Tibshirani. Surprises in high-dimensional ridgeless least squares interpolation. *arXiv preprint arXiv:1903.08560*, 2019.

[28] Michal Derezinski, Feynman T Liang, and Michael W Mahoney. Exact expressions for double descent and implicit regularization via surrogate random design. *Advances in neural information processing systems*, 33:5152–5164, 2020.

[29] Jeffrey Pennington and Yasaman Bahri. Geometry of neural network loss surfaces via random matrix theory. In *International Conference on Machine Learning*, pages 2798–2806. PMLR, 2017.

[30] Alexander Wei, Wei Hu, and Jacob Steinhardt. More than a toy: Random matrix models predict how real-world neural representations generalize. *arXiv preprint arXiv: Arxiv-2203.06176*, 2022.

[31] Chiyuan Zhang, Samy Bengio, Moritz Hardt, Benjamin Recht, and Oriol Vinyals. Understanding deep learning (still) requires rethinking generalization. *Communications of the ACM*, 64(3):107–115, 2021.

[32] Gintare Karolina Dziugaite, Alexandre Drouin, Brady Neal, Nitarshan Rajkumar, Ethan Caballero, Linbo Wang, Ioannis Mitliagkas, and Daniel M Roy. In search of robust measures of generalization. *Advances in Neural Information Processing Systems*, 33:11723–11733, 2020.

[33] Yurii Nesterov. *Introductory lectures on convex optimization: A basic course*, volume 87. Springer Science & Business Media, 2003.

[34] Tomaso Poggio, Gil Kur, and Andrzej Banburski. Double descent in the condition number. *arXiv preprint arXiv:1912.06190*, 2019.

[35] Jaehoon Lee, Yasaman Bahri, Roman Novak, Samuel S Schoenholz, Jeffrey Pennington, and Jascha Sohl-Dickstein. Deep neural networks as gaussian processes. *arXiv preprint arXiv:1711.00165*, 2017.

[36] Arthur Jacot, Franck Gabriel, and Clément Hongler. Neural tangent kernel: Convergence and generalization in neural networks. *Advances in neural information processing systems*, 31, 2018.

[37] Jeff Cheeger. A lower bound for the smallest eigenvalue of the laplacian. *Problems in analysis*, Princeton Univ. Press, Princeton, N. J.,:pp. 195–199., 1970.

[38] Sridhar Mahadevan and Mauro Maggioni. Proto-value functions: A laplacian framework for learning representation and control in markov decision processes. *J. Mach. Learn. Res.*, 8:2169–2231, 2007.

[39] Marlos C. Machado, Marc G. Bellemare, and Michael Bowling. A Laplacian framework for option discovery in reinforcement learning. In Doina Precup and Yee Whye Teh, editors, *Proceedings of the 34th International Conference on Machine Learning*, volume 70 of *Proceedings of Machine Learning Research*, pages 2295–2304. PMLR, 06–11 Aug 2017.

[40] Marlos C. Machado, Clemens Rosenbaum, Xiaoxiao Guo, Miao Liu, Gerald Tesauro, and Murray Campbell. Eigenoption discovery through the deep successor representation. In *6th International Conference on Learning Representations, ICLR 2018, Vancouver, BC, Canada, April 30 - May 3, 2018, Conference Track Proceedings*. OpenReview.net, 2018.

[41] Yifan Wu, George Tucker, and Ofir Nachum. The laplacian in rl: Learning representations with efficient approximations. *arXiv preprint arXiv:1810.04586*, 2018.

[42] Jinho Baik, Gérard Ben Arous, and Sandrine Péché. Phase transition of the largest eigenvalue for nonnull complex sample covariance matrices. *The Annals of Probability*, 33(5):1643–1697, 2005.

[43] Gene H Golub. Some modified matrix eigenvalue problems. *SIAM review*, 15(2):318–334, 1973.

[44] Léon Bottou and Olivier Bousquet. The tradeoffs of large scale learning. In J. Platt, D. Koller, Y. Singer, and S. Roweis, editors, *Advances in Neural Information Processing Systems*, volume 20. Curran Associates, Inc., 2007.

[45] Bruno Scherrer. Should one compute the temporal difference fix point or minimize the bellman residual? the unified oblique projection view. *arXiv preprint arXiv:1011.4362*, 2010.

[46] Richard S Sutton and Andrew G Barto. *Reinforcement learning: An introduction*. MIT press, 2018.

[47] Richard S Sutton, Doina Precup, and Satinder Singh. Between mdps and semi-mdps: A framework for temporal abstraction in reinforcement learning. *Artificial intelligence*, 112(1-2):181–211, 1999.

[48] Charles Bordenave, Pietro Caputo, and Djalil Chafaï. Circular law theorem for random markov matrices. *Probability Theory and Related Fields*, 152(3):751–779, 2012.

[49] Stéphane Boucheron, Gábor Lugosi, and Pascal Massart. *Concentration inequalities: A nonasymptotic theory of independence*. Oxford university press, 2013.

[50] Terence Tao. *Topics in random matrix theory*, volume 132. American Mathematical Soc., 2012.

[51] Andrei Z Broder and Anna R Karlin. Bounds on the cover time. *Journal of Theoretical Probability*, 2(1):101–120, 1989.

[52] Romain Couillet and Zhenyu Liao. *Random Matrix Methods for Machine Learning: When Theory meets Applications*. 2021.

Checklist

1. For all authors...
   (a) Do the main claims made in the abstract and introduction accurately reflect the paper's contributions and scope? [Yes]
   (b) Did you describe the limitations of your work? [Yes]
   (c) Did you discuss any potential negative societal impacts of your work? [N/A] This work is a theoretical model for TD(0) in the linear setting. As such we do not think there are any applications with a societal impact to be foreseen.
   (d) Have you read the ethics review guidelines and ensured that your paper conforms to them? [Yes]
2. If you are including theoretical results...

(a) Did you state the full set of assumptions of all theoretical results? [Yes] Some finer details can be found in the proofs in appendices.
(b) Did you include complete proofs of all theoretical results? [Yes] Statements such as Lemmas or propositions have a full proof in appendix. Informal statements and approximations have a derivation in appendix where we make clear what the approximation/asssumption is.

3. If you ran experiments...
   (a) Did you include the code, data, and instructions needed to reproduce the main experimental results (either in the supplemental material or as a URL)? [Yes] Colab notebooks are supplied to reproduce the figures.
   (b) Did you specify all the training details (e.g., data splits, hyperparameters, how they were chosen)? [Yes]
   (c) Did you report error bars (e.g., with respect to the random seed after running experiments multiple times)? [Yes]
   (d) Did you include the total amount of compute and the type of resources used (e.g., type of GPUs, internal cluster, or cloud provider)? [N/A] Used public Colab notebook compute.
4. If you are using existing assets (e.g., code, data, models) or curating/releasing new assets...
   (a) If your work uses existing assets, did you cite the creators? [N/A]
   (b) Did you mention the license of the assets? [N/A]
   (c) Did you include any new assets either in the supplemental material or as a URL? [N/A]
   (d) Did you discuss whether and how consent was obtained from people whose data you're using/curating? [N/A]
   (e) Did you discuss whether the data you are using/curating contains personally identifiable information or offensive content? [N/A]
5. If you used crowdsourcing or conducted research with human subjects...
   (a) Did you include the full text of instructions given to participants and screenshots, if applicable? [N/A]
   (b) Did you describe any potential participant risks, with links to Institutional Review Board (IRB) approvals, if applicable? [N/A]
   (c) Did you include the estimated hourly wage paid to participants and the total amount spent on participant compensation? [N/A]

A Appendix: Experiments

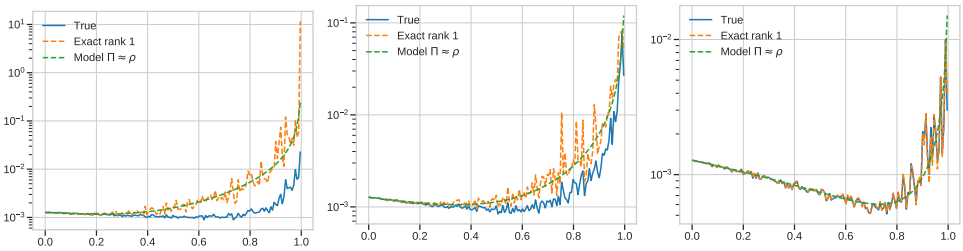

(a) $\mathbf{P}^\pi$ (b) $\mathbf{P}^\pi \triangleq \left(\mathbf{P}^\pi\right)^5$ (c) $\mathbf{P}^\pi \triangleq \left(\mathbf{P}^\pi\right)^{25}$

Figure 4: We plot the estimation error (in blue), the exact asymptotic model when $\hat{\mathbf{P}}^\pi$ becomes rank 1 (orange) in Section 4.3 and its simplification (green). On the x axis we have the ratio p/n and on the y axis we have the value of the estimation error.

On Figure 4 we test the models developed in Section 4.3. Note that the models were developed for a $\hat{\mathbf{P}}^\pi$ approximately rank 1. We can see on (a) that the models, both the exact and the simplified overestimate the true estimation error in a 14×14 4 rooms domain ($n = 784$) for various $p = 1 \dots n$.

However, if we were to do something akin to a k-step return, where we consider one action to be a sequence of k, this would be equivalent to changing $\hat{\mathbf{P}}^\pi$ to $\left(\hat{\mathbf{P}}^\pi\right)^k$. In (b) and (c) we can see that taking a higher k improve our estimation. Taking powers of the transition matrix has for effect to push down all the eigenvalues < 1 and as such make the graph "better" connected. All in all, while our formula is not precise in a realistic scenario, when considering an iterated setting, it recovers the estimation precisely.

Note that for Figure 4 we chose not to average over random Φ as it highlights the exactness of the rank one model developed in Section 4.3.

B Appendix: Proofs

In the paper and in the proofs, we extend naturally the notation $o(\cdot)$ to matrices with the following definition

$$\mathbf{A} \in o(1) \iff \|\mathbf{A}\| \in o(\|1\|)$$

for $\|\cdot\|$ a natural operator norm. In this paper we only consider the 2-operator norm which corresponds to the largest singular value.

B.1 Deformed random graph

In Section 2.3 we derive informally an expression for the Markov transition matrix of a random graph taking into account $\mathbf{d}_\pi$. Let us go into more details here, and explain why we called it an *informal* derivation. Let us recall that $\mathbf{A}^\pi = n\mathbf{A}\mathbf{D}_\pi$ for $\mathbf{A}$ the original adjacency matrix and $\mathbf{D}_\pi = \texttt{diag}(\mathbf{d}_\pi)$ the stationary distribution of π. To get $\hat{\mathbf{P}}^\pi$ we need to normalize the rows $i = 1, \dots n$ of $\mathbf{A}^\pi$ by their sum, i.e the degree d_i of each state.

In the uniform case, $\mathbf{A}^\pi = \mathbf{A}$, [48] provide first a sketch of proof (eq 1.6) based on the fact that $d_i = \mathbf{D}_{ii} = \sum_j \mathbf{A}_{ij}$ satisfies $|d_i - n\mu| \in o(n)$ by the law of large numbers. This allows to "replace" $\mathbf{D}$ by $n\mu\mathbf{I}_n$ in the proofs which ties it back to the general Wigner/i.i.d case.

In the deformed case, we cannot invoke directly the law of large numbers. Indeed, now $d_i = \sum_j \mathbf{A}^\pi_{ij} = n\sum_j \mathbf{A}_{ij}\mathbf{d}_\pi(j)$ so we have a weighted sum instead of a simple one.

We need a concentration inequality for the weighted sum of random variables. One can be found in [49]

Lemma B.1 (From [49])**.** *Let $X_1, X_2, \dots, X_n$ be iid copies of a real random variable X that obeys, for some $p \geq 1$*

$$\mathbb{P}(|X| > u) \leq \exp\left(-u^p\right)$$

for all $u > 0$. Then there exists $L > 0$ such that, for any $s \in \mathbb{R}^n$, and for q the conjugate of p ($\frac{1}{p} + \frac{1}{q} = 1$)

$$\mathbb{P}\left(\sum_{i=1}^n s_i X_i > t\right) \leq L\exp\left(-\frac{1}{L}\min\{\frac{t^p}{\|s\|_p^q}, \frac{t^2}{\|s\|_2^2}\}\right)$$

In our case, for $X_j = c \cdot (\mathbf{A}_{ij} - \mu)$ (where c is chosen so the the tail assumption is satisfied),

$$\mathbb{P}(\sum_j \mathbf{d}_\pi(j)(\mathbf{A}_{ij} - \mu) > t) \leq L\exp\left(-\frac{1}{L}\min\{\frac{(ct)^p}{\|\mathbf{d}_\pi\|_p^q}, \frac{(ct)^2}{\|\mathbf{d}_\pi\|_2^2}\}\right)$$

$$\mathbb{P}(\frac{d_i}{n} - \mu > t) \leq L\exp\left(-\frac{1}{L}\min\{\frac{(ct)^p}{\|\mathbf{d}_\pi\|_p^q}, \frac{(ct)^2}{\|\mathbf{d}_\pi\|_2^2}\}\right)$$

Thus, if $\|\mathbf{d}_\pi\|_p^q$ and $\|\mathbf{d}_\pi\|_2^2$ are $\in o(1)$, and then reasoning on $-X_j$ we have that $|\frac{d_i}{n} - \mu|$ is, almost surely when n is large, smaller than any constant $t > 0$, therefore $o(1)$. Thus we get the same argument $\mathbf{D} = n\mu\mathbf{I}_n + o(n)$. Note here that in high dimension the stronger condition for $\mathbf{d}_\pi$ will be

for $p = \infty$, $\|\mathbf{d}_\pi\|_\infty \in o(1)$. As we already make a stronger assumption later, we have chosen not to include it in the main text.

All of this allows to calculate $\hat{\mathbf{P}}^\pi$ by normalizing $\mathbf{A}^\pi$

$$\begin{aligned}\hat{\mathbf{P}}^\pi &= \mathbf{D}^{-1}\mathbf{A}^\pi \\ &\approx (\frac{1}{n\mu})n\mathbf{A}\mathbf{D}_\pi \\ &= (\frac{1}{\mu})(\mu\mathbf{1}_n\mathbf{1}_n^\top + \sigma\mathbf{W})\mathbf{D}_\pi \\ &= \mathbf{1}_n\mathbf{d}_\pi^\top + \frac{\sigma}{\mu}\mathbf{W}\mathbf{D}_\pi\end{aligned}$$

When the entries of $\mathbf{A}$ are iid Bernoulli of mean μ, we have $\sigma^2 = \mu(1-\mu)$ and $\mathbf{W}$ has iid whitened Bernoulli entries.

We consider this proof informal as there are a certain number of technicalities involved when controlling the deviation of all these random quantities (as we have sketched above for the expected degree).

B.2 Asymptotically well-connected graph

Proposition 3.1. *For the $\mathbf{d}_\pi$-deformed $\mathbb{G}(n,\mu)$ graph studied above, assuming $\hat{\mathbf{P}}^\pi = \mathbf{1}_n\mathbf{d}_\pi^\top + \mathbf{X}^\pi$, then the graph is asymptotically well-connected if $n\|\mathbf{d}_\pi\|_\infty \in o(\sqrt{d})$.*

Proof. First, recall that

$$\mathbf{X}^\pi = \sqrt{\frac{n(1-\mu)}{\mu}}\tfrac{1}{\sqrt{n}}\mathbf{W}\mathbf{D}_\pi$$

For $\|\cdot\|$ the 2-operator corresponding to the maximum singular value, we have:

$$\|\mathbf{X}^\pi\| \leq \sqrt{\frac{n(1-\mu)}{\mu}}\|\tfrac{1}{\sqrt{n}}\mathbf{W}\|\|\mathbf{D}_\pi\|$$

From [50] we have for both Wigner (Corollary 2.3.6), when the graph is undirected and i.i.d matrices (Corollary 2.3.5) when the edges are iid and directed, that There exists $A, C, c > 0$

$$\mathbb{P}(\|\tfrac{1}{\sqrt{n}}\mathbf{W}\| \geq A) \leq C\exp(-cn)$$

Which can be understood as $\frac{1}{\sqrt{n}}\mathbf{W}$ has bounded operator norm with overwhelming probability. In particular, taking the limit $n \to \infty$ gives us that $\frac{1}{\sqrt{n}}\mathbf{W}$ has bounded norm almost surely when $n \to \infty$.

Then $\|\mathbf{D}_\pi\| = \|\mathbf{d}_\pi\|_\infty$ where $\|\cdot\|_\infty$ is the vector max-norm. This is due to the fact that $\mathbf{D}_\pi$ is a diagonal matrix with positive entries, therefore its largest singular value is its largest eigenvalue.

For $\|\mathbf{X}^\pi\|$ to be $o(1)$ we need

$$\sqrt{\frac{n(1-\mu)}{\mu}} \cdot \|\mathbf{d}_\pi\|_\infty \cdot \|\tfrac{1}{\sqrt{n}}\mathbf{W}\| \in o(1)$$

As $1-\mu \leq 1$ and for $n\mu = d$, it is sufficient to have (almost surely)

$$n\|\mathbf{d}_\pi\|_\infty \in o(\sqrt{d})$$

□

Lemma B.2. *From [51], for a irreducible and aperiodic Markov transition matrix $\mathbf{P}^\pi$, we have that, for ${\mathbf{P}^\pi}^k_{ij} = \mathbf{d}_{\pi j} + O(\sqrt{\frac{\mathbf{d}_{\pi j}}{\mathbf{d}_{\pi i}}}\lambda_2^k)$, thus*

$$\mathbf{P}^k = \mathbf{1}\mathbf{d}_\pi^\top + O(\sqrt{\kappa(\mathbf{d}_\pi)}\lambda_2^k)$$

where $\kappa(\cdot)$ is the condition number.

This lemma means that when using longer back-ups, as is for instance done when using n-step returns, the second eigenvalue of $\mathbf{P}^k$ will shrink to 0 as long as $1 \in o(k)$.

B.3 Spiked Marchenko-Pastur distribution

For, we prove small result showing that the $o(1)$ appearing in $\hat{\mathbf{P}}^\pi$ remains a $o(1)$ in $\frac{1}{n}\Phi^\top(\mathbf{I}_n - \gamma\hat{\mathbf{P}}^\pi)\Phi$.

Lemma B.3. *For $\hat{\mathbf{P}}^\pi$ satisfying the asymptotically well-connected condition, we have*

$$\frac{1}{n}\Phi^\top(\mathbf{I}_n - \gamma\hat{\mathbf{P}}^\pi)\Phi = \frac{1}{n}\Phi^\top(\mathbf{I}_n - \gamma\mathbf{1}_n\mathbf{d}_\pi^\top)\Phi + o(1)$$

Proof. For $\|\cdot\| = \|\cdot\|_2$ the 2-operator norm which corresponds to the largest singular value, we have

$$\begin{aligned}\frac{1}{n}\|\Phi^\top o(1)\Phi\| &\leq \frac{1}{n}\|\Phi\|^2 \cdot \|o(1)\| \\ &= \frac{1}{n}\left(\sqrt{\lambda_{\max}(\Phi^\top\Phi)}\right)^2 o(1)\end{aligned}$$

As the maximum eigenvalue of $\frac{1}{n}\Phi^\top\Phi$ converges a.s to $(1+\sqrt{\rho})^2$ per the Marchenko-Pastur theorem

$$\frac{1}{n}\|\Phi^\top o(1)\Phi\| \xrightarrow{a.s} o(1)$$

□

This lemma is a useful result to understand that a $o(1)$ perturbation stays a $o(1)$ perturbation when adding features.

Proposition B.1 (Asymmetric rank 1 perturbation)**.** *We consider the spectrum of $\frac{1}{n}\Phi^\top(\mathbf{I}_n - \gamma\mathbf{u}\mathbf{v}^\top)\Phi$ for $\mathbf{u}, \mathbf{v} \in \mathbb{R}^n$ so that $\mathbf{v}^\top\mathbf{u} = 1$ and $\gamma \in [0, 1[$ which is a rank 1 perturbation of the Wishart covariance model. If $\rho\gamma^2 < 1$ the spectrum of $\frac{1}{n}\Phi^\top(\mathbf{I}_n - \gamma\mathbf{u}\mathbf{v}^\top)\Phi$ converges to the Marchenko-Pastur law. When $\rho\gamma^2 \geq 1$, the empirical spectral distribution also converges to the Marchenko-Pastur law, but additionally, we observe a phase transition [42], and an eigenvalue λ^{spiked} separates from the bulk*

$$\boxed{\lambda^+_{\min} \xrightarrow[p/n\to\rho]{a.s} \lambda^{spiked} = (1-\gamma)(\rho - \tfrac{1}{\gamma})} \tag{14}$$

Proof. The proof is based on a simple adaptation of the proof in [52] (page 117). As we consider an asymmetric spike, we lose commutative properties. Thus, we can only prove our result in the case where there is a unique spike instead of a finite number as is usual. We are looking to characterize the eigenvalues of $\frac{1}{n}\Phi^\top(\mathbf{I}_n - \gamma\mathbf{u}\mathbf{v}^\top)\Phi$, or equivalently (up to some zeros), the eigenvalues of $\frac{1}{n}\Phi\Phi^\top(\mathbf{I}_n - \gamma\mathbf{u}\mathbf{v}^\top)$. However, in this case, $\frac{1}{n}\Phi\Phi^\top$ is not a sample from the Wishart distribution, but $\frac{1}{p}\Phi\Phi^\top$ is. We therefore analyze $\frac{1}{p}\Phi\Phi^\top$ and will simply have to scale our spectrum by ρ at the end.

$$\begin{aligned}0 &= \det\left(\frac{1}{p}\Phi\Phi^\top(\mathbf{I}_n - \gamma\mathbf{u}\mathbf{v}^\top) - \hat{\lambda}\mathbf{I}_n\right) \\ 0 &= \det\left(\frac{1}{p}\Phi\Phi^\top - \hat{\lambda}(\mathbf{I}_n - \gamma\mathbf{u}\mathbf{v}^\top)^{-1}\right)\det(\mathbf{I}_n - \gamma\mathbf{u}\mathbf{v}^\top)\end{aligned}$$

Using Sherman-Morrison formula, we have $(\mathbf{I}_n - \gamma \mathbf{u}\mathbf{v}^\top)^{-1} = \mathbf{I}_n + \frac{\gamma}{1-\gamma}\mathbf{u}\mathbf{v}^\top$ as $\mathbf{v}^\top \mathbf{u} = 1$.

Since $\det\left(\mathbf{I}_n - \gamma \mathbf{u}\mathbf{v}^\top)\right) \neq 0$, the second determinant can be discarded. Then, we can factor the resolvent of the Wishart model. That is, letting $\mathbf{Q}(\hat{\lambda}) = \left(\frac{1}{p}\Phi\Phi^\top - \hat{\lambda}\mathbf{I}_n\right)^{-1}$, we write

$$\begin{aligned} 0 &= \det\left(\tfrac{1}{p}\Phi\Phi^\top - \hat{\lambda}\mathbf{I}_n - \hat{\lambda}\frac{\gamma}{1-\gamma}\mathbf{u}\mathbf{v}^\top\right) \\ &= \det \mathbf{Q}^{-1}(\hat{\lambda}) \det\left(\mathbf{I}_n - \hat{\lambda}\mathbf{Q}(\hat{\lambda})\frac{\gamma}{1-\gamma}\mathbf{u}\mathbf{v}^\top\right). \end{aligned}$$

Inverting $\frac{1}{p}\Phi\Phi^\top - \hat{\lambda}\mathbf{I}_n$ is almost surely possible when $\hat{\lambda} < (1 - \sqrt{1/\rho})^2$ per the concentration of the empirical spectral distribution of Wishart covariance models to the Marchenko-Pastur law and the term $\mathbf{Q}^{-1}(\hat{\lambda})$ is almost surely non-zero. So the left term can be discarded. For the second we use Sylvester's determinant identity to end up with a scalar equation

$$0 = \left(1 - \hat{\lambda}\mathbf{v}^\top \mathbf{Q}(\hat{\lambda})\mathbf{u}\frac{\gamma}{1-\gamma}\right).$$

As $\mathbf{Q}(\hat{\lambda})$ is a deterministic equivalent of $m(\hat{\lambda})\mathbf{I}_n$ ([18], Theorem 2.4 in [52]), where $m(\cdot)$ is the Stieljes transform of the MP distribution, thus

$$\hat{\lambda}\mathbf{v}^\top \mathbf{Q}(\hat{\lambda})\mathbf{u}\frac{\gamma}{1-\gamma} = \hat{\lambda}m(\hat{\lambda})\frac{\gamma}{1-\gamma} + o(1)$$

The above determinant is zero when

$$\hat{\lambda}m(\hat{\lambda}) = \frac{1-\gamma}{\gamma} + o(1) \tag{15}$$

□

From the definition of $m(\cdot)$ as the Stieljes transform of the MP distribution, we know [52] it satisfies

$$zm(z) = -1 + \frac{1}{1 - z - czm(z)}$$

for $c = \lim n, p \to \infty n/p = 1/\rho$ Thus, for $z = \hat{\lambda}$

$$\hat{\lambda} = 1 - c\hat{\lambda}m(\hat{\lambda}) - \frac{1}{1 + \hat{\lambda}m(\hat{\lambda})}$$

Plugging the equation above, asymptotically

$$\begin{aligned} \hat{\lambda} &= 1 - c\frac{1-\gamma}{\gamma} - \frac{1}{1 + \frac{1-\gamma}{\gamma}} \\ &= 1 - c\frac{1-\gamma}{\gamma} - \gamma \\ &= (1-\gamma)(1 - \frac{1}{\rho\gamma}) \end{aligned}$$

Now, we have to remember to multiply our spectrum by ρ to obtain the original one, and so we obtain

$$\boxed{\hat{\lambda} = (1-\gamma)(\rho - \frac{1}{\gamma})}$$

When $(1-\gamma)(\rho - \frac{1}{\gamma}) \leq (1 - \sqrt{\rho})^2$ which is equivalent to $\rho\gamma^2 \geq 1$, this eigenvalue is isolated on the left of the bulk.

Proposition 3.2 (Spiked MP). *If $\rho\gamma^2 < 1$ the spectrum of $\frac{1}{n}\Phi^\top(\mathbf{I}_n - \gamma\hat{\mathbf{P}}^\pi)\Phi$ converges to the Marchenko-Pastur law with parameter ρ. When $\rho\gamma^2 \geq 1$, there is a phase transition [42] for the minimum non-zero eigenvalue $\lambda^+_{\min}$ which separates from bulk and converges to*

$$\boxed{\lambda^+_{\min} \xrightarrow[p/n\to\rho]{a.s} \lambda^{spiked} = (1-\gamma)(\rho - \tfrac{1}{\gamma})} \tag{6}$$

Proof. We essentially do the same proof as above, but with an additional $o(1)$ moving around and we show that it does not impact the Stieljes transform, thus the spectrum, almost surely.

$$0 = \det\left(\frac{1}{n}\Phi\Phi^\top(\mathbf{I}_n - \gamma\hat{\mathbf{P}}^\pi) - \hat{\lambda}\mathbf{I}_n\right)$$
$$0 = \det\left(\frac{1}{n}\Phi\Phi^\top(\mathbf{I}_n - \gamma\mathbf{1}_n\mathbf{d}_\pi^\top + o(1)) - \hat{\lambda}\mathbf{I}_n\right)$$

Where we used the definition of $\hat{\mathbf{P}}^\pi$ and Lemma B.3. Then

$$0 = \det\left(\frac{1}{n}\Phi\Phi^\top - \hat{\lambda}(\mathbf{I}_n - \gamma\mathbf{1}_n\mathbf{d}_\pi^\top + o(1))^{-1}\right)\det(\mathbf{I}_n - \gamma\mathbf{1}_n\mathbf{d}_\pi^\top + o(1))$$

As the eigenvalues of $\mathbf{I}_n - \gamma\mathbf{1}_n\mathbf{d}_\pi^\top$ are lower bounded by $1-\gamma$ for n large enough $\det(\mathbf{I}_n - \gamma\mathbf{1}_n\mathbf{d}_\pi^\top + o(1))$ must be non-zero. As $(\mathbf{I}_n + o(1))^{-1} = \sum_i (o(1))^i = \mathbf{I}_n + o(1)$, using Sherman-Morrison formula, we have $(\mathbf{I}_n + o(1) - \gamma\mathbf{1}_n\mathbf{d}_\pi^\top)^{-1} = \mathbf{I}_n + o(1) + o(1)\frac{\gamma(1+o(1))}{1-\gamma+o(1)}\mathbf{1}_n\mathbf{d}_\pi^\top = \mathbf{I}_n + \frac{\gamma}{1-\gamma}\mathbf{1}_n\mathbf{d}_\pi^\top + o(1)$ as $\mathbf{d}_\pi^\top\mathbf{1}_n = 1$

With the same derivation and arguments as above

$$\begin{aligned} 0 &= \det\left(\frac{1}{n}\Phi\Phi^\top - \hat{\lambda}\mathbf{I}_n - \hat{\lambda}\frac{\gamma}{1-\gamma}\mathbf{1}_n\mathbf{d}_\pi^\top + o(1)\right) \\ &= \det\mathbf{Q}^{-1}(\hat{\lambda})\det\left(\mathbf{I}_n - \hat{\lambda}\mathbf{Q}(\hat{\lambda})\big(\frac{\gamma}{1-\gamma}\mathbf{1}_n\mathbf{d}_\pi^\top + o(1)\big)\right). \end{aligned}$$

And finally we end up with the same equality as before where the $o(1)$ from the perturbation and the one from the deterministic equivalent fuse together. As the determinant is continuous

$$\hat{\lambda}\mathbf{d}_\pi^\top\mathbf{Q}(\hat{\lambda})\mathbf{1}_n\frac{\gamma}{1-\gamma} = \hat{\lambda}m(\hat{\lambda})\frac{\gamma}{1-\gamma} + o(1)$$

Therefore the Stieljes transforms when using $\hat{\mathbf{P}}^\pi$ and $\mathbf{1}_n\mathbf{d}_\pi^\top$ are asymptotically the same, thus, almost surely, they have the same empirical spectral distribution.

□

B.4 Approximation of the extreme eigenvalues

Lemma 3.1. *If $\Xi = \texttt{diag}(\xi_1, \ldots, \xi_n)$ is non-singular, the eigenvalues of $\Xi(\mathbf{I}_n - \gamma\mathbf{1}_n\mathbf{d}_\pi^\top)$ satisfy a* secular *equation [43]*

$$1 - \gamma\sum_{i=1}^n \frac{\xi_i \cdot \mathbf{d}_\pi(i)}{\xi_i - \lambda} = 0 \tag{7}$$

Proof. Let us consider $\mathbf{v} \neq 0$ and λ, an eigenvector of $\Xi(\mathbf{I}_n - \gamma\mathbf{1}_n\mathbf{d}_\pi^\top)$ and its associated eigenvalue.

$$\lambda\mathbf{v} = \Xi(\mathbf{I}_n - \gamma\mathbf{1}_n\mathbf{d}_\pi^\top)\mathbf{v}$$

This give on component i

$$\lambda v_i = \xi_i v_i - \gamma \xi_i \sum_j \mathbf{d}_\pi(j) v_j$$

Then

$$\gamma \xi_i \sum_j \mathbf{d}_\pi(j) v_j = (\xi_i - \lambda) v_i$$

Assuming $\lambda \neq \xi_i, \forall i$

$$\gamma \frac{\xi_i \sum_j \mathbf{d}_\pi(j) v_j}{\xi_i - \lambda} = v_i$$

Multiplying by $\mathbf{d}_\pi(i)$ and summing

$$\gamma \sum_i \frac{\mathbf{d}_\pi(i) \xi_i \cdot \sum_j \mathbf{d}_\pi(j) v_j}{\xi_i - \lambda} = \sum_i \mathbf{d}_\pi(i) v_i$$

Now the same term $\sum_j \mathbf{d}_\pi(j) v_j = \mathbf{d}_\pi^\top \mathbf{v}$ appears on both sides. Let us verify if it can be null. If that were the case, we would have $\Xi(\mathbf{I}_n - \gamma \mathbf{1}_n \mathbf{d}_\pi^\top)\mathbf{v} = \Xi \mathbf{v} = \lambda \mathbf{v}$. Thus, as Ξ is diagonal, the possible vectors $\mathbf{v}$ possible are the canonical basis vectors and the possible eigenvalues are ξ_i. However, as $\mathbf{d}_\pi$ is a positive vector whose entries sum to 1, we cannot have $\mathbf{d}_\pi^\top \mathbf{v} = 0$. Thus $\mathbf{d}_\pi^\top \mathbf{v} \neq 0$ and by dividing on each side:

$$\gamma \sum_i \frac{\xi_i \mathbf{d}_\pi(i)}{\xi_i - \lambda} = 1$$

□

B.5 Optimization and approximation error

Lemma 4.1 (Decomposition of the error)**.** *For $\mathbf{q}_t = \Phi \theta_t$, where θ_t is updated with TD(0) (eq.* (2)*), we have the following decomposition*

$$\|\mathbf{r} + \gamma \mathbf{P}^\pi \mathbf{q}_t - \mathbf{q}_t\|_\Xi \leq \sqrt{n \|\Xi\|_\infty} \cdot \|\mathbf{q}_t - \mathbf{q}_{TD}\|_2 + \|\mathbf{r} + \gamma \mathbf{P}^\pi \mathbf{q}_{TD} - \mathbf{q}_{TD}\|_\Xi \tag{10}$$

where $\|\mathbf{x}\|_\Xi = \sqrt{\mathbf{x}^\top \Xi \mathbf{x}}$ is the 2-norm in metric Ξ.

Proof.

$$\begin{aligned}
\|\mathbf{r} + \gamma \mathbf{P}^\pi \mathbf{q}_t - \mathbf{q}_t\|_\Xi &= \|\gamma \mathbf{P}^\pi (\mathbf{q}_t - \mathbf{q}_{\text{TD}}) - (\mathbf{q}_t - \mathbf{q}_{\text{TD}}) + \mathbf{r} + \gamma \mathbf{P}^\pi \mathbf{q}_{\text{TD}} - \mathbf{q}_{\text{TD}}\|_\Xi \\
&\leq \|\gamma \mathbf{P}^\pi (\mathbf{q}_t - \mathbf{q}_{\text{TD}}) - (\mathbf{q}_t - \mathbf{q}_{\text{TD}})\|_\Xi + \|\mathbf{r} + \gamma \mathbf{P}^\pi \mathbf{q}_{\text{TD}} - \mathbf{q}_{\text{TD}}\|_\Xi \\
&= \sqrt{(\mathbf{q}_t - \mathbf{q}_{\text{TD}})^\top (\mathbf{I}_n - \gamma \mathbf{P}^\pi)^\top \Xi (\mathbf{I}_n - \gamma \mathbf{P}^\pi)(\mathbf{q}_t - \mathbf{q}_{\text{TD}})} + \|\mathbf{r} + \gamma \mathbf{P}^\pi \mathbf{q}_{\text{TD}} - \mathbf{q}_{\text{TD}}\|_\Xi \\
&\leq \|\sqrt{\Xi}(\mathbf{I}_n - \gamma \mathbf{P}^\pi)\|_2 \|\mathbf{q}_t - \mathbf{q}_{\text{TD}}\|_2 + \|\mathbf{r} + \gamma \mathbf{P}^\pi \mathbf{q}_{\text{TD}} - \mathbf{q}_{\text{TD}}\|_\Xi \\
&\leq \|\sqrt{\Xi}\|_2 \cdot \|\mathbf{I}_n - \gamma \mathbf{P}^\pi\|_2 \|\mathbf{q}_t - \mathbf{q}_{\text{TD}}\|_2 + \|\mathbf{r} + \gamma \mathbf{P}^\pi \mathbf{q}_{\text{TD}} - \mathbf{q}_{\text{TD}}\|_\Xi \\
&\leq \sqrt{\|\xi\|_\infty} \sqrt{n} \|\mathbf{I}_n - \gamma \mathbf{P}^\pi\|_\infty \|\mathbf{q}_t - \mathbf{q}_{\text{TD}}\|_2 + \|\mathbf{r} + \gamma \mathbf{P}^\pi \mathbf{q}_{\text{TD}} - \mathbf{q}_{\text{TD}}\|_\Xi \\
&\leq \sqrt{\|\xi\|_\infty} \sqrt{n} \|\mathbf{q}_t - \mathbf{q}_{\text{TD}}\|_2 + \|\mathbf{r} + \gamma \mathbf{P}^\pi \mathbf{q}_{\text{TD}} - \mathbf{q}_{\text{TD}}\|_\Xi
\end{aligned}$$

Where we used $\|\mathbf{A}\|_2 \leq \sqrt{n} \|\mathbf{A}\|_\infty$ and the fact that $\mathbf{P}^\pi$ is a stochastic matrix, thus has entries between 0 and 1. As such, the entries of $\mathbf{I}_n - \gamma \mathbf{P}^\pi$ are between $-\gamma$ and 1, in particular they are bounded by 1. □

Proposition 4.1. *Let us assume that $\Phi^\top \Xi(\mathbf{I}_n - \gamma \mathbf{P}^\pi)\Phi$ is diagonalizable as $\mathbf{Q}\Lambda\mathbf{Q}^{-1}$, and that its spectrum is real and positive. Denoting by $\lambda^+_{\min}$ and $\lambda_{\max}$ its smallest non-zero and largest eigenvalues, for $\eta = \frac{2}{\lambda^+_{\min}+\lambda_{\max}}$*

$$\|\mathbf{q}_t - \mathbf{q}_{TD}\|_2^2 \leq \left(\frac{\lambda_{\max}/\lambda^+_{\min} - 1}{\lambda_{\max}/\lambda^+_{\min} + 1}\right)^{2t} K^2 \|\mathbf{q}_0 - \mathbf{q}_{TD}\|_2^2 \tag{11}$$

where $K = \kappa(\Phi)\kappa(\mathbf{Q})$ when $p < n$ and $K = \kappa(\mathbf{Q})$ when $p > n$ where κ is the condition number.

Proof. Let us begin with the case $p > n$ From the TD iteration Equation (2) multiplied on the left by Φ

$$\mathbf{q}_{t+1} = \Phi\Phi^\top \Xi \mathbf{r} - \Phi\Phi^\top \Xi(\mathbf{I}_n - \gamma \mathbf{P}^\pi)\mathbf{q}_t$$

For a i.i.d matrix Φ, we have that $\Phi\Phi^\top$ is almost surely invertible. Thus the fixed point of this iteration is

$$\begin{aligned}
\mathbf{q}_{\text{TD}} &= \left(\Phi\Phi^\top \Xi(\mathbf{I}_n - \gamma \mathbf{P}^\pi)\right)^{-1} \Phi\Phi^\top \Xi \mathbf{r} \\
&= \left(\mathbf{I}_n - \gamma \mathbf{P}^\pi\right)^{-1} \Xi^{-1} (\Phi\Phi^\top)^{-1} \Phi\Phi^\top \Xi \mathbf{r} \\
&= \left(\mathbf{I}_n - \gamma \mathbf{P}^\pi\right)^{-1} \mathbf{r} \\
&= \mathbf{q}^\pi
\end{aligned}$$

Thus, for $\mathbf{H}_{\text{TD}} = \Phi^\top \Xi(\mathbf{I}_n - \gamma \mathbf{P}^\pi)\Phi$ and $\mathbf{x}_t = \mathbf{q}_t - \mathbf{q}^\pi$

$$\begin{aligned}
\|\mathbf{x}_t\|_2^2 &= \|(\mathbf{I}_n - \eta \mathbf{H}_{\text{TD}})^t \mathbf{x}_0\|_2^2 \\
&\leq \|(\mathbf{I}_n - \mathbf{H}_{\text{TD}})^t\|_2^2 \|\mathbf{x}_0\|_2^2 \\
&= \|\mathbf{Q}(\mathbf{I}_n - \eta\Lambda)^t \mathbf{Q}^{-1}\|_2^2 \|\mathbf{x}_0\|_2^2 \\
&\leq \|\mathbf{Q}\|_2^2 \|\mathbf{Q}^{-1}\|_2^2 \|(\mathbf{I}_n - \eta\Lambda)^t\|_2^2 \|\mathbf{x}_0\|_2^2 \\
&= \kappa(\mathbf{Q})^2 \max_{i, \lambda_i = \Lambda_{ii}} \{|1 - \eta\lambda_i|\}^{2t} \|\mathbf{x}_0\|_2^2
\end{aligned}$$

As $\mathbf{I}_n - \eta\Lambda$ is diagonal, and as such its largest singular value (2-norm) is its largest eigenvalue (in modulus).

Now, we supposed the eigenvalues were real, $\max_{i,\lambda_i=\Lambda_{ii}}\{|1 - \eta\lambda_i|\}$ will be minimized when the largest and smallest terms are equal.

$$|1 - \eta\lambda^+_{\min}| = |1 - \eta\lambda_{\max}|$$

If $\lambda^+_{\min} = \lambda_{\max}$ this can be achieved for any η, however the only solution when they are different is to have the two expressions above of a different sign

$$1 - \eta\lambda^+_{\min} = -1 + \eta\lambda_{\max}$$

Which leads to $\eta = \frac{2}{\lambda^+_{\min}+\lambda_{\max}}$ and

$$|1 - \eta\lambda^+_{\min}| = |1 - \eta\lambda_{\max}| = \frac{\lambda_{\max} - \lambda^+_{\min}}{\lambda_{\max} + \lambda^+_{\min}}$$

Now for $p < n$ we do a similar reasoning with θ. By the exact same reasoning, but using $\mathbf{H}_{\text{TD}} = \Phi^\top \Xi(\mathbf{I}_n - \gamma \mathbf{P}^\pi)\Phi$ instead and the fixed point $\theta_{\text{TD}} = \big(\Phi^\top \Xi(\mathbf{I}_n - \gamma \mathbf{P}^\pi)\Phi\big)^1 \Phi^\top \Xi \mathbf{r}$ we get

$$\|\theta_t - \theta_{\text{TD}}\| \leq \kappa(\mathbf{Q})^2 \big(\frac{\lambda_{\max} - \lambda^+_{\min}}{\lambda_{\max} + \lambda^+_{\min}}\big)^{2t} \|\theta_0 - \theta_{\text{TD}}\|_2^2$$

Now, we would like to obtain a result for the Q-function associated to these parameters. We have $\sigma_{\min}(\Phi)\|\mathbf{x}\|_2 \leq \|\Phi\mathbf{x}\|_2 \leq \sigma_{\max}(\Phi)\|\mathbf{x}\|_2$ for $\sigma_{\max}$ and $\sigma_{\min}$ the max and min singular values. Thus, multiplying each side by $\sigma_{\min}(\Phi)\sigma_{\max}(\Phi)$, we get

$$\sigma_{\min}(\Phi)\|\mathbf{q}_t - \mathbf{q}_{\text{TD}}\| \leq \sigma_{\min}(\Phi)\sigma_{\max}(\Phi)\|\theta_t - \theta_{\text{TD}}\|$$

and

$$\sigma_{\min}(\Phi)\sigma_{\max}(\Phi)\|\theta_0 - \theta_{\text{TD}}\|_2 \leq \sigma_{\max}(\Phi)\|\mathbf{q}_0 - \mathbf{q}_{\text{TD}}\|$$

Squaring these results and putting it back in the contraction equation, we get for $\mathbf{q}_{\text{TD}} = \Phi\theta_{\text{TD}}$

$$\begin{aligned}
\|\mathbf{q}_t - \mathbf{q}_{\text{TD}}\|^2 &\leq \kappa(\mathbf{Q})^2 \big(\frac{\lambda_{\max} - \lambda^+_{\min}}{\lambda_{\max} + \lambda^+_{\min}}\big)^{2t} \big(\frac{\sigma_{\max}(\Phi)}{\sigma_{\min}(\Phi)}\big)^2 \|\mathbf{q}_0 - \mathbf{q}_{\text{TD}}\|_2^2 \\
&= \kappa(\mathbf{Q})^2 \big(\frac{\lambda_{\max} - \lambda^+_{\min}}{\lambda_{\max} + \lambda^+_{\min}}\big)^{2t} \kappa(\Phi)^2 \|\mathbf{q}_0 - \mathbf{q}_{\text{TD}}\|_2^2
\end{aligned}$$

□

B.6 Peaking behavior of the estimation error

Proposition 4.2. *Let us assume $\hat{\mathbf{P}}^\pi$ satisfies the well-connected property, i.e that it is asymptotically rank one*

$$\lim_{\substack{n,p\to\infty \\ p/n\to\rho}} \|(\mathbf{I}_n - \gamma\hat{\mathbf{P}}^\pi)\mathbf{q}_{TD} - \mathbf{r}\|_\Xi^2 = \|\Pi_\perp \mathbf{r}\|_\Xi^2 + \frac{2\gamma}{1-\gamma\tilde{\rho}}(\mathbf{d}_\pi^\top \Pi\mathbf{r})(\xi^\top \Pi_\perp \mathbf{r}) + (\frac{\gamma}{1-\gamma\tilde{\rho}})^2 \xi^\top \Pi_\perp \mathbf{1}_n (\mathbf{d}_\pi^\top \Pi\mathbf{r})^2$$

where Π is the orthogonal projector onto the span of Φ in norm Ξ: $\Pi = \Phi(\Phi^\top\Xi\Phi)^{-1}\Phi^\top\Xi$, $\Pi_\perp = \mathbf{I}_n - \Pi$ is its complement, and $\tilde{\rho} = \mathbf{d}_\pi^\top \Pi \mathbf{1}_n$.

Proof. Let us look at the case $p < n$. We have $\mathbf{q}_{\text{TD}} = \Phi\big(\Phi^\top\Xi(\mathbf{I} - \gamma\mathbf{P}^\pi)\Phi\big)^{-1}\Phi^\top\Xi\mathbf{r}$ We will therefore study more closely the matrix $\Phi\big(\Phi^\top\Xi(\mathbf{I} - \gamma\mathbf{P})\Phi\big)^{-1}\Phi^\top\Xi$, in the case where $\mathbf{P}^\pi = \mathbf{u}\mathbf{v}^\top$ is a rank one matrix. First, Sherman-Morrison formula gives us

$$(\mathbf{A} - \gamma\mathbf{x}\mathbf{y}^\top)^{-1} = \mathbf{A}^{-1} + \gamma\frac{\mathbf{A}^{-1}\mathbf{x}\mathbf{y}^\top\mathbf{A}^{-1}}{1 - \gamma\mathbf{y}^\top\mathbf{A}^{-1}\mathbf{x}}$$

which is the usual formula but for $\mathbf{x} \triangleq -\gamma\mathbf{x}$. Note that this is licit as long as $1 - \gamma\mathbf{y}^\top\mathbf{A}^{-1}\mathbf{x} \neq 0$. Using Sherman-Morrison's formula

$$\begin{aligned}
\Phi\big(\Phi^\top\Xi(\mathbf{I} - \gamma\mathbf{P}^\pi)\Phi\big)^{-1}\Phi^\top\Xi &= \Phi\big(\Phi^\top\Xi\Phi - \gamma\Phi^\top\Xi\mathbf{u}\mathbf{v}^\top\Phi\big)^{-1}\Phi^\top\Xi \\
&= \Phi\big(\Phi^\top\Xi\Phi - \gamma\Phi^\top\Xi\mathbf{u}(\Phi^\top\mathbf{v})^\top\big)^{-1}\Phi^\top\Xi \\
&= \Phi\big((\Phi^\top\Xi\Phi)^{-1} + \gamma\frac{(\Phi^\top\Xi\Phi)^{-1}\Phi^\top\Xi\mathbf{u}(\Phi^\top\mathbf{v})^\top(\Phi^\top\Xi\Phi)^{-1}}{1 - \gamma\mathbf{v}^\top\Phi(\Phi^\top\Xi\Phi)^{-1}\Phi^\top\Xi\mathbf{u}}\big)\Phi^\top\Xi \\
&= \Phi(\Phi^\top\Xi\Phi)^{-1}\Phi^\top\Xi + \gamma\frac{\Phi(\Phi^\top\Xi\Phi)^{-1}\Phi^\top\Xi\mathbf{u}\mathbf{v}^\top\Phi(\Phi^\top\Xi\Phi)^{-1}\Phi^\top\Xi}{1 - \gamma\mathbf{v}^\top\Phi(\Phi^\top\Xi\Phi)^{-1}\Phi^\top\Xi\mathbf{u}} \\
&= \Phi(\Phi^\top\Xi\Phi)^{-1}\Phi^\top\Xi + \gamma\frac{\Phi(\Phi^\top\Xi\Phi)^{-1}\Phi^\top\Xi\mathbf{u}\mathbf{v}^\top\Phi(\Phi^\top\Xi\Phi)^{-1}\Phi^\top\Xi}{1 - \gamma\mathbf{v}^\top\Phi(\Phi^\top\Xi\Phi)^{-1}\Phi^\top\Xi\mathbf{u}} \\
&= \Pi + \gamma\frac{\Pi\mathbf{u}\mathbf{v}^\top\Pi}{1 - \gamma\mathbf{v}^\top\Pi\mathbf{u}}
\end{aligned}$$

For $\Pi = \Phi(\Phi^\top \Xi \Phi)^{-1}\Phi^\top \Xi$ the usual projector unto the span of Φ in metric Ξ.

Now, for the TD error we obtain

$$
\begin{aligned}
(\mathbf{I} - \gamma \mathbf{P}^\pi)\mathbf{q}_{\text{TD}} - \mathbf{r} &= (\mathbf{I} - \gamma \mathbf{P}^\pi)\big(\Pi + \gamma \frac{\Pi \mathbf{u}\mathbf{v}^\top \Pi}{1 - \gamma \mathbf{v}^\top \Pi \mathbf{u}}\big)\mathbf{r} - \mathbf{r} \\
&= \big(\Pi + \gamma \frac{\Pi \mathbf{u}\mathbf{v}^\top \Pi}{1 - \gamma \mathbf{v}^\top \Pi \mathbf{u}} - \gamma \mathbf{P}^\pi \Pi - \gamma \mathbf{u}\mathbf{v}^\top \gamma \frac{\Pi \mathbf{u}\mathbf{v}^\top \Pi}{1 - \gamma \mathbf{v}^\top \Pi \mathbf{u}}\big)\mathbf{r} - \mathbf{r} \\
&= \big(\Pi + \gamma \frac{\Pi \mathbf{u}\mathbf{v}^\top \Pi}{1 - \gamma \mathbf{v}^\top \Pi \mathbf{u}} - \gamma \mathbf{u}\mathbf{v}^\top \Pi - \gamma^2 \mathbf{v}^\top \Pi \mathbf{u} \frac{\mathbf{u}\mathbf{v}^\top \Pi}{1 - \gamma \mathbf{v}^\top \Pi \mathbf{u}}\big)\mathbf{r} - \mathbf{r} \\
&= \big(\Pi + \gamma \frac{\Pi \mathbf{u}\mathbf{v}^\top \Pi}{1 - \gamma \mathbf{v}^\top \Pi \mathbf{u}} - \gamma \frac{\mathbf{u}\mathbf{v}^\top \Pi}{1 - \gamma \mathbf{v}^\top \Pi \mathbf{u}}\big)\mathbf{r} - \mathbf{r} \\
&= \big(\Pi - \mathbf{I} + \gamma \frac{(\Pi - \mathbf{I})\mathbf{u}\mathbf{v}^\top \Pi}{1 - \gamma \mathbf{v}^\top \Pi \mathbf{u}}\big)\mathbf{r} \\
&= (\Pi - \mathbf{I})\big(\mathbf{I} + \frac{\gamma}{1 - \gamma \mathbf{v}^\top \Pi \mathbf{u}} \mathbf{u}\mathbf{v}^\top \Pi\big)\mathbf{r}
\end{aligned}
$$

Let's call $\mathbf{I} - \Pi = \Pi_\perp$ the complement projector projector and $\tilde{\rho} = \mathbf{v}^\top \Pi \mathbf{u}$. Now, for the MSBE error, we get

$$
\begin{aligned}
\|(\mathbf{I} - \gamma \mathbf{P})\mathbf{q}_{\text{TD}} - \mathbf{r}\|_\Xi^2 &= \mathbf{r}^\top \big(\mathbf{I} + \frac{\gamma}{1 - \gamma \tilde{\rho}} \mathbf{u}\mathbf{v}^\top \Pi\big)^\top (\Pi - \mathbf{I})^\top \Xi \big(\Pi - \mathbf{I}\big)\big(\mathbf{I} + \frac{\gamma}{1 - \gamma \tilde{\rho}} \mathbf{u}\mathbf{v}^\top \Pi\big)\mathbf{r} \\
&= \mathbf{r}^\top \big(\mathbf{I} + \frac{\gamma}{1 - \gamma \tilde{\rho}} \Pi^\top \mathbf{v}\mathbf{u}^\top\big)\Pi_\perp^\top \Xi \Pi_\perp \big(\mathbf{I} + \frac{\gamma}{1 - \gamma \tilde{\rho}} \mathbf{u}\mathbf{v}^\top \Pi\big)\mathbf{r} \\
&= \mathbf{r}^\top \big(\Pi_\perp^\top \Xi \Pi_\perp + \frac{\gamma}{1 - \gamma \tilde{\rho}} \Pi^\top \mathbf{v}\mathbf{u}^\top \Xi \Pi_\perp + \Pi_\perp^\top \Xi \frac{\gamma}{1 - \gamma \tilde{\rho}} \mathbf{u}\mathbf{v}^\top \Pi + \frac{\gamma}{1 - \gamma \tilde{\rho}} \Pi^\top \mathbf{v}\mathbf{u}^\top \Xi \Pi_\perp \frac{\gamma}{1 - \gamma \tilde{\rho}} \mathbf{u}\mathbf{v}^\top \Pi\big)\mathbf{r} \\
&= \|\Pi_\perp \mathbf{r}\|_\Xi^2 + \frac{2\gamma}{1 - \gamma \tilde{\rho}} (\mathbf{v}^\top \Pi \mathbf{r})(\xi^\top \Pi_\perp \mathbf{r}) + \big(\frac{\gamma}{1 - \gamma \tilde{\rho}}\big)^2 (\mathbf{v}^\top \Pi \mathbf{r})^2 (\xi^\top \Pi \mathbf{u})
\end{aligned}
$$

where we use the fact that $\Pi^\top \Xi \Pi = \Xi \Pi = \Pi^\top \Xi$ and same for $\Pi_\perp$.

Using $\mathbf{v} = \mathbf{d}_\pi$ and $\mathbf{u} = \mathbf{1}_n$ gives us the approximation.

□

C Colab links

For plotting the spiked MP spectra `https://colab.research.google.com/drive/1E3DgmZQF1-1FNYeVo4msyGUHwRiK32WE?usp=sharing`

For the extreme eigenvalues approximation `https://colab.research.google.com/drive/1H_GkjzlGyUxB0i55jM5VAqLXoEGGxN3h?usp=sharing`

For the peaking behavior `https://colab.research.google.com/drive/1EVudyGfieXOUqDLifdhFrs8Pu1OzKOAW?usp=sharing`

For the peaking behavior model `https://colab.research.google.com/drive/1pLIqaV5BO1ChIj9y9UmP5jmlWx26FNI7?usp=sharing`

For the unstability wrt η and ϵ `https://colab.research.google.com/drive/1CuPZhv3eZoINXHCKLtwjVlHrLy9ylBuI?usp=sharing`